

“Photocatalytic water splitting to produce hydrogen using visible light active photocatalyst”

Thesis on
“Photocatalytic water splitting to produce hydrogen using
visible light active photocatalyst”

Jadavpur University
Department of Chemical Engineering

Submitted by
SOURAV CHAULE
Class Roll no.- 001710302014
Exam. Roll No.- M4CHE19010
Registration No.- 140621 of 2017-2018
Session: 2017-2019
Master of Chemical Engineering

Project Supervisor:
Prof. Kajari Kargupta

This project report is submitted towards the completion of
Master of Engineering degree in Chemical Engineering.

Acknowledgement

I would like express my gratitude for the help, cooperation and inspiration that I have received from my teachers, friends and well-wishers during this course. It is their kind help and untiring effort that has resulted in completion of this project.

I thank God Almighty for all His blessings.

I am highly obliged and grateful to my Project Coordinator **Prof. Kajari Kargupta**, for her excellent guidance, endless encouragement and cooperation extended to me, right from the time of onset of this task till its successful completion.

I am very grateful to **Prof. Debashis Roy**, Head of the Department, Chemical Engineering Department for all the necessary help I got during my project work.

I am also indebted to Jadavpur University, Dept. of Chemical Engineering for supporting me and giving me the opportunity to use the equipment's to do my research.

My sincere appreciation also extends to all my lab mates and especially my mentor **Miss Arundhati Sarkar**, who have provided assistance at various occasions; however, it is not possible to list all of them in this limited space.

I would also like to extend my thanks to our Lab assistant **Mr. Ajay Kumar Prodhan** and my colleague **Mr. Sayantanu Mandal** who have helped me lot throughout my work.

I am grateful to my parents and all of my family members who encouraged and supported me all through and helped me in all respect.

.....

Sourav Chaule

CERTIFICATION

This is to certify that Mr. Sourav Chaule, final year Master of Chemical Engineering (M.ChE) examination student of Department of Chemical Engineering, Jadavpur University, Examination Roll No M4CHE19010, Registration No 140621 of 2017-2018 has completed the Project work titled, **“Photocatalytic water splitting to produce hydrogen using visible light active photocatalyst”** under the guidance of **Prof. Kajari Kargupta** during his Masters Curriculum. This work has not been reported earlier anywhere and can be approved for submission in partial fulfillment of the course work.

.....
Prof. Debashis Roy

Head of the Department and Professor

Chemical Engineering Department

Jadavpur University

.....
Prof. Kajari Kargupta

Project Supervisor

Professor, Chemical Engineering Department

Jadavpur University

.....
SIGNATURE OF DEAN

Abstract

Photocatalytic water splitting is an alternative way compared to the other conventional routes for hydrogen generation. However, the major drawbacks of this process are i) slow kinetics ii) high recombination rate of photo-generated electrons and holes iii) less retention time for the reaction iv) low yield of production

Here, these issues are addressed employing two approaches:

i) A visible light active hybrid water adsorbent-semiconductor photo-catalyst: CdS-Sodium Alginate that boosts the fast adsorption and allows high retention time, is synthesized, characterized and tested.

ii) Reduced Graphene oxide based hybrid CdS-Sodium Alginate photo-catalyst promoting the electron transport and decreasing the recombination rate, is synthesized, characterized and examined.

Sodium alginate having different functional groups likes hydroxyl and carboxyl group is used as active center for water adsorption. Band gap energy of hybrid CdS-Sodium Alginate photo-catalyst is 3 eV which is little bit higher than pristine CdS, so rate of recombination decreases and gives better photo-catalytic activity (4021 μ mole/gm hour) than pristine CdS (3169 μ mole/gm hour). Further combination of rGO with hybrid CdS-Sodium Alginate provides more surface area and promotes the electron transport that enhances the photo-catalytic activity (5001 μ mole/gm hour) for 10 mg of catalyst loading without any co-catalyst.

Both powder and spherical beads of hybrid CdS-Sodium Alginate and rGO-CdS-Sodium Alginate are synthesized by different techniques and characterized using SEM, FTIR, XRD and UV-VIS spectroscopy. Water splitting is performed using laboratory scale photo-reactor in semi batch mode of operation with 100 watt LED lamp. Further, for the first time remarkably enhanced the photocatalytic activity (6029 μ mole/gm/hour, for 40 mg optimum catalyst loading) is achieved using rGO based water adsorbent mediated visible light active photo-catalyst without any co-catalyst.

CONTENTS

Chapter-1 Introduction

- 1.1 Introduction
- 1.2 Importance of hydrogen energy
- 1.3 Different routes of hydrogen production
- 1.4 Photo-chemical water splitting under visible light
 - 1.4.1 Advantages of photocatalytic hydrogen generation
 - 1.4.2 Concept and general principle of photocatalytic hydrogen generation
 - 1.4.3 Different configuration of photo-chemical water splitting
 - 1.4.4 Energy requirements
 - 1.4.5 Material requirements
 - 1.4.6 Operating condition affecting the photocatalytic hydrogen generation

Chapter-2 Literature review and Aim & Objective

- 2.1 Introduction
 - 2.1.1 Summary of the literature review
 - 2.1.2 Process bottle necks
- 2.2 Role of adsorbent on photocatalytic water splitting
- 2.3 Role of Graphene on photocatalytic hydrogen generation
- 2.4 Research gap
- 2.5 Aim and Objective of the Project
 - 2.5.1 The aim of the project work
 - 2.5.2 Role of CdS
 - 2.5.3 Role of Sodium alginate
- 2.6 The specific objectives of the project work

Chapter-3 Experimental work and Methodology

- 3.1 Synthesis of different visible light active photo-catalyst
- 3.2 Characterization of different photo-catalyst
- 3.3 Study of adsorption characteristic of different adsorbents
- 3.4 Generation of hydrogen using synthesized photo-catalyst: Performance analysis

- 3.5 Comparative analysis of activity of different synthesized photo-catalysts
- 3.6 Study of role of catalyst loading on the rate of production of hydrogen
- 3.7 Kinetic study of photocatalytic water splitting
- 3.8 Study on Recyclability of the photo-catalyst

Chapter-4 Result and discussion

- 4.1 Characterization of different synthesized photo-catalyst
 - 4.1.1 Structural characterization: Scanning electron microscopy (SEM)
 - 4.1.2 Identification of groups: Fourier transformed infrared spectroscopy (FTIR)
 - 4.1.3 Crystallinity: X-ray diffraction (XRD)
 - 4.1.4 Spectrophotometric characterization: UV-VIS spectroscopy: Band gap calculation
- 4.2 Experimental result
 - 4.2.1 Study of adsorption characteristic of different water adsorbents
 - 4.2.2 Generation of hydrogen using synthesized photo-catalyst: Performance analysis
 - 4.2.3 Comparative analysis of activity of different synthesized photo-catalysts
 - 4.2.4 Study of role of catalyst loading on the rate of production of hydrogen
 - 4.2.5 Kinetic study of photocatalytic water splitting
 - 4.2.6 Study on Recyclability of the photo-catalyst

Chapter-5 Conclusion

- 5.1 Conclusion

Chapter-6 References

List of figures

Fig-1.1 Total installed power generation capacity (end of April 2017)

Fig-1.2 Mechanism of photocatalytic water splitting

Fig-1.3 Photo-electro-catalytic water splitting

Fig-1.4 Photocatalytic water splitting

Fig-2.1 Properties of Graphene

Fig-2.2 3D network of Graphene

Fig-2.3 Polymer network sodium-alginate

Fig-3.1 Process flow diagram of CdS synthesis

Fig-3.2 Process flow diagram of hybrid CdS-Sodium alginate

Fig-3.3 KMnO_4

Fig-3.4 Graphite flakes

Fig-3.5 Stirring for 8 hrs

Fig-3.6 Termination step

Fig-3.7 Different stages of washing

Fig-3.8 Filtration

Fig-3.9 Drying

Fig-3.10 Process flow diagram of rGO-CdS-Sodium alginate

Fig-3.11 Tauc plot

Fig-3.12 Experimental setup

Fig-4.1 Representative SEM images of CdS nanocatalyst

Fig-4.2 EDAX spectrum of CdS nanocatalyst

Fig-4.3 Representative SEM images of hybrid CdS-Sodium alginate nanocatalyst

Fig-4.4 EDAX spectrum of hybrid CdS-Sodium alginate nano-catalyst

Fig-4.5 Representative SEM images of rGO-CdS-Sodium alginate photo-catalyst

Fig-4.6 EDAX spectrum of rGO-CdS-Sodium alginate photo-catalyst

Fig-4.7 FTIR images of CdS/ CdS-Sodium alginate and rGO-CdS-Sodium alginate photo-catalyst

Fig-4.8 The XRD pattern of CdS/ hybrid CdS-Sodium alginate and rGO-CdS-Sodium alginate

Fig-4.9 UV-VIS spectroscopy of different synthesized catalyst: Pristine CdS/ hybrid CdS-Sodium alginate and rGO-CdS-Sodium alginate

Fig-4.10 Moisture adsorbed/mass of adsorbent (x/m) vs temperature plot

Fig-4.11 Moles of hydrogen generated vs time plot using Pristine CdS with 10 mg of catalyst loading

Fig-4.12 Moles of hydrogen generated vs time plot using hybrid CdS-Sodium alginate with 10 mg of catalyst loading

Fig-4.13 Moles of hydrogen generated vs time plot using rGO-CdS-Sodium alginate with 10 mg of catalyst loading

Fig-4.14 Comparative representation: Moles of hydrogen vs time plot using pristine CdS/ hybrid CdS-Sodium alginate and rGO-CdS-Sodium alginate with 10 mg of catalyst loading

Fig-4.15 Activity plot of different synthesized photo-catalysts

Fig-4.16 Moles of hydrogen generated vs time plot using rGO-CdS-Sodium alginate with different catalyst loading

Fig-4.17 Photocatalytic activity plot of hybrid rGO-CdS-Sodium alginate with different loading

Fig-4.18 Concentration vs time plot

Fig-4.19 $1/(-r_A)$ vs $1/C_A$ plot

Fig- 4.20 Concentration vs time plot

Fig-4.21 $(-1/r_A)$ vs $1/C_A$ plot

Fig- 4.22 ($-1/r_A$) vs $1/C_A$ plot in a splitting manner

Fig-4.23 Effect of catalyst deactivation on moles of hydrogen generation for rGO-CdS-Sodium alginate

CHAPTER I

Introduction

Photo-catalytic water splitting to produce hydrogen using visible light active photo-catalyst

1.1 Introduction

The progressively serious energy crisis and the environmental pollution caused by the burning of fossil fuels have led to a hard-hitting search for renewable and environmental friendly alternative energy recourses. [1] The world's population growth and the continuous expansion of the manufacturing sector are two main observable factors of this increased energy requirements. A number of recent studies suggest that the direct use of hydrogen as a fuel may provide a much cleaner and far less expensive fuel alternative. Almost no pollution is produced by engines that burn hydrogen. So, hydrogen energy has been recognized as a potentially significant alternative form of storable and clean energy for the future. Nowadays, hydrogen is being produced in large quantities for industrial and commercial purpose. Most of hydrogen production however, requires fossil fuels. It largely uses steam to reform natural gas; it utilizes electrolysis from electricity which can be produced from natural gas, coal, petroleum feedstock or nuclear energy. According to natural resources, 15.9% of India's total energy production comes from renewable sources. [2]

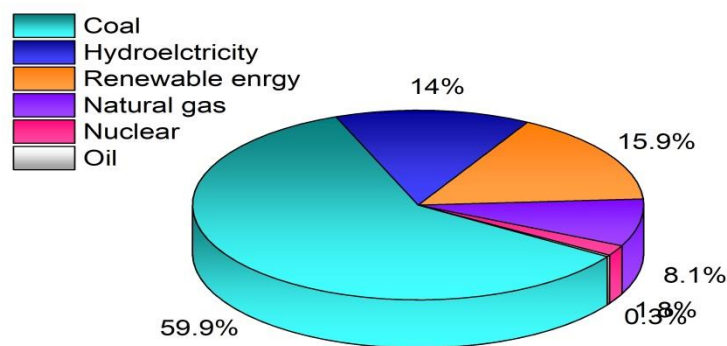


Fig-1.1 Total installed power generation capacity (end of April 2017)

Thus nowadays challenge is to produce hydrogen from renewable resources. In this respect, hydrogen can be considered as a secondary energy carrier, being produced first from other

alternative renewable feedstock. There are so many advantages and disadvantages to manufacture hydrogen from renewable sources that is shown in the table-1.

Advantages	Technology	Disadvantages
<ul style="list-style-type: none"> ✓ Abundant ✓ Cheap material ✓ Use of water or organic sources 	Solar-hydrogen	<ul style="list-style-type: none"> ○ Clear sky is required ○ Conversion efficiency
<ul style="list-style-type: none"> ✓ Sunlight use ✓ Excess energy may be provided 	Photovoltaic	<ul style="list-style-type: none"> ○ Expensive technology ○ Requires clear sky
<ul style="list-style-type: none"> ✓ Operates day/night 	Wind power	<ul style="list-style-type: none"> ○ High cost ○ Exposition to high wind
<ul style="list-style-type: none"> ✓ Provides water/power ✓ Day/night operation 	Hydroelectric	<ul style="list-style-type: none"> ○ Require lot of water
<ul style="list-style-type: none"> ✓ Constant operation day/night 	Tidal power	<ul style="list-style-type: none"> ○ Limited to coasts
	Geothermal power	<ul style="list-style-type: none"> ○ Limited access to geothermal activity
	Biomass	<ul style="list-style-type: none"> ○ Green gases are emitted

Table-1: Common renewable energy technologies

Water, a natural storehouse of hydrogen, can be utilized to yield hydrogen for commercial purpose in the near future. In this context, photo-catalytic water splitting, a simple and cost-effective approach to generate hydrogen seems quite favorable. Photo-catalytic water splitting involves the splitting of water into hydrogen and oxygen using a semiconductor catalyst upon irradiation of light. Since the first report on photo-catalytic splitting of water on TiO₂ electrodes was published in 1972 by Honda and Fujishima [3], photo-catalysis has shown wide-range of application from environmental to energy application. The research on the photo-catalytic splitting of water to produce hydrogen, mirrors the natural photosynthesis phenomena by converting solar energy into chemical energy, has been carried on extensively. Recently researchers have been focusing on the development of visible-light-responsive photo-catalysts,

because the ultraviolet (UV) light only accounts for about 4% of the solar radiation energy, while the visible light contributes to about 43%.

1.2 Importance of hydrogen energy

Hydrogen can be considered as clean energy carriers as similar to electricity. Hydrogen can be produced by various resources such as renewable and nuclear energy. In the long term hydrogen will simultaneously reduce the dependence of foreign oil and the emission of green- house gases and other pollutants.

➤ Hydrogen as an energy carrier

Hydrogen can be considered as secondary source of energy, commonly referred to as an energy carrier. Energy carriers are used to move, store and deliver energy in a form that can be easily used. Electricity is most well-known example of energy carrier. Hydrogen is an important energy carrier and in the future it will be utilized for having a number of advantages. For example, a large volume of hydrogen energy can be stored in a number of different ways. [4] Hydrogen is also considered as high efficiency, low polluting fuel that can be used for transportation, heating and power generation in places where it is difficult to use electricity. In some instances, it is cheaper to ship hydrogen by pipeline than sending electricity over long distances by wire.

➤ The future of hydrogen

In the future, hydrogen will join electricity as an important energy carrier, since it can be made safely from renewable energy sources and is virtually non-polluting. It will also be used as a fuel for 'zero-emissions' vehicles, to heat home and offices, to produce electricity, and to fuel air craft. Hydrogen has greater potential as a way to reduce reliance on imported energy sources such as oil. Before hydrogen can play a bigger role and become a widely used alternative to gasoline, many new facilities and system must be built.

1.3 Different routes of hydrogen generation

Molecular hydrogen is not available on earth in convenient natural reservoirs. Most hydrogen on earth is bounded to oxygen and water. Manufacturing elemental hydrogen does require consumption of hydrogen carrier such as a fossil fuel or water. The former consumes the fossil resource and produce carbon-dioxide, but often requires no further energy input beyond the fossil fuel. Decomposing water requires electrical or heat input, generated from some primary energy sources. The energy source has to provide all of the energy that is available from the hydrogen

fuel, as well as all of that lost due to inefficiency during both the production and consumption of the hydrogen.

I. Thermochemical Process

Some thermal processes use the energy in various resources, such as natural gas, coal and biomass to release hydrogen from their molecular structure. In other process heat in combination with closed-chemical cycles produces hydrogen from feedstock such as water.

- Natural gas reforming (SMR)
- Coal gasification
- Bio-mass gasification
- Biomass-derived liquid reforming
- Solar thermochemical hydrogen (STCH)

II. Electro-lytic Process

Electrolyzers use electricity to split water into oxygen and water. The technology is well developed and available commercially and systems that can efficiently use intermittent renewable power and being developed.

III. Direct solar water splitting process

Direct solar water splitting or photo-catalytic processes use light energy to split water into hydrogen and oxygen. These processes are currently in the very early stages of research but offer long-term potential for sustainable hydrogen production with low environmental impact.

- Photo-catalytic water splitting
- Photo-electro-catalytic water splitting

IV. Biological Process

Microbes such as bacteria and micro-algae can produce hydrogen through biological reactions, using sunlight or organic matter. These technology pathways are at an early stage of research but in the long-term have the potential for sustainable, low-carbon hydrogen production.

- Microbial bio-mass conversion
- Photo-biological

1.4 Photo-chemical water splitting

1.4.1 Advantage of Photo-catalytic hydrogen generation

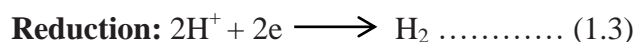
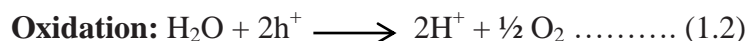
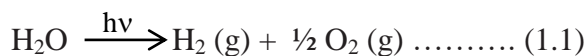
Photo-catalytic water splitting is an inexpensive and clean route of hydrogen production compared to others conventional routes. Photo-catalytic water splitting has been attracting significant interest in the recent literature because it uses two of the most abundant sources, clean, renewable and natural energy resources available to us.

Advantages at a glance:

- Hydrogen production from renewable sources (water)
- Available light source (solar energy)
- No GHG emission (environment friendly)
- Simple experimental set-up for hydrogen production
- Economic process

1.4.2 General principle of photocatalytic water splitting

Photochemical water splitting, like other photo-catalytic processes, is initiated when a photo-semiconductor absorbs light photons with energies greater than its band-gap energy (E_g). This absorption creates excited photoelectrons in the conduction band (CB) and holes in the valence band (VB) of the semiconductor, as schematically depicted in Figure-1.2. [5] As indicated in Fig-1.2 once the photo-generated electron-hole pairs have been created in the semiconductor bulk, they must separate and migrate to the surface competing effectively with the electron-hole recombination process that consumes the photo-charges generating heat. At the surface of the semiconductor, the photo induced electrons and holes reduce and oxidize adsorbed water to produce gaseous oxygen and hydrogen by the following reactions:



Water splitting into H_2 and O_2 is classified as an “up-hill” photo-catalytic reaction because it is accompanied by a large positive change in the Gibbs free energy ($\Delta G^0=237 \text{ kJ mol}^{-1}$, 2.46 eV per molecule). [6] In this reaction, photon energy is converted into chemical energy (hydrogen energy), as seen in photosynthesis by green plants. This reaction is therefore sometimes referred to as artificial photosynthesis.

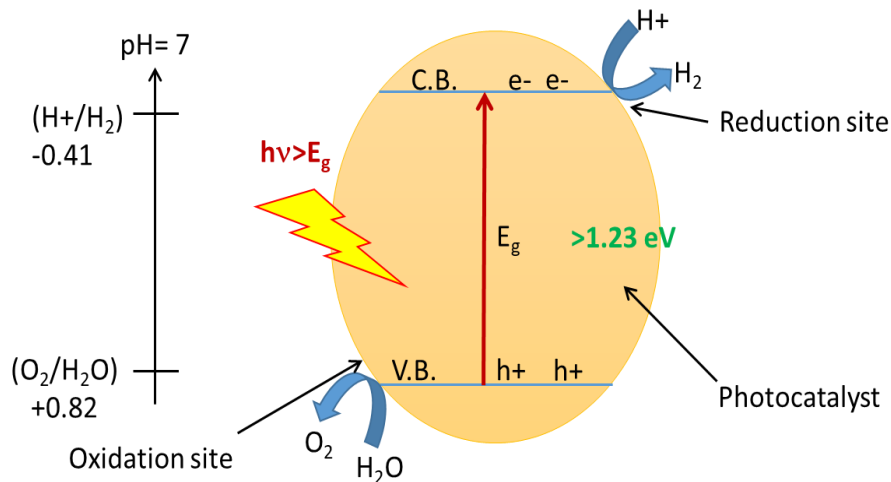


Fig-1.2 Mechanism of photocatalytic water splitting

1.4.3 Configuration

Photo-catalysts for photochemical water splitting can be used for this purpose according to two types of configurations: (i) photo-electrochemical cells and (ii) photo-catalytic systems. [5]

Photo-electrochemical configuration: The photo-electrochemical cell for water decomposition (Figure 1.3) involves two electrodes immersed in an aqueous electrolyte, of which one is a photo-catalyst exposed to light (photo-anode in Figure 1.3). The photo-generated electron-hole pairs, produced as a result of light absorption on the photo-anode, are separated by an electric field within the semiconductor. On the one hand, the photo-generated holes migrate to the surface of the semiconductor where they oxidize water molecules to oxygen. [5]

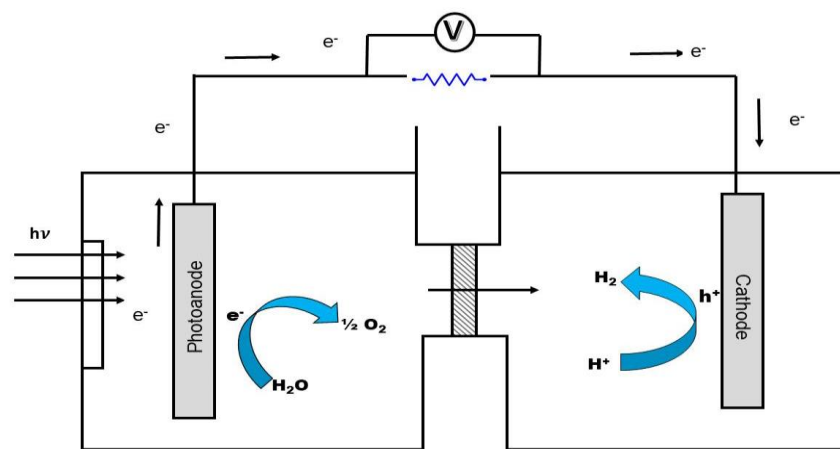


Fig-1.3 Photo-electro-catalytic water splitting

On the other hand, the photo-generated electrons move through an electrical circuit to the counter electrode and there reduce H^+ to hydrogen. In order to achieve practical current densities, an additional potential driving-force is usually required through the imposition of external bias voltage or the imposition of an internal bias voltage by using different concentrations of hydrogen ions in the anode/ cathode compartments. Water splitting using a photo-electrochemical cell was first reported by Fujishima and Honda using an electrochemical system consisting of a TiO_2 semiconductor electrode connected through an electrical load to a platinum black counter electrode. [5] Photo-irradiation of the TiO_2 electrode under a small electric bias leads to the evolution of H_2 and O_2 at the surface of the Pt counter electrode and TiO_2 photo-electrode, respectively.

Photo-catalytic configuration: The principles of photochemical water splitting can be extended to the design of systems using photo-catalytic semiconductors in the form of particles or powders suspended in aqueous solutions. In this system, each photo-catalyst particle functions as a micro-photo-electrode performing both oxidation and reduction of water on its surface (Figure 1.4). Such particulate systems have the advantage of being much simpler and less expensive to develop and use than photo-electrochemical cells.

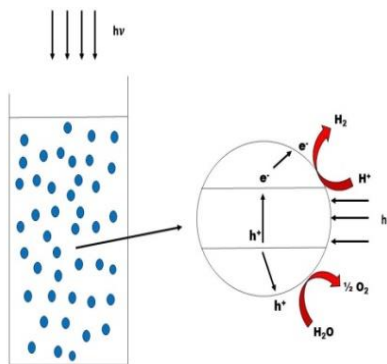


Fig-1.4 Photocatalytic water splitting

Furthermore, a wide variety of materials can be used as photo-catalysts in particulate systems. These particulates may be rather difficult to prepare in the form of single crystals or in form of high-quality polycrystalline phases which are necessary in the case of photo-electrodes. Another advantage is that electrical conductivity does not need to be as high as that required by photo-electrodes. Moreover, the efficiency of light absorption in suspensions or slurries of powders can be very high because of the high semiconductor surface exposed to light. For instance, 100mg of

the photo-catalyst powder of particle diameter ~ 0.1 μm consists of more than 10^{11} particles that are mobile and independent of each other. However, particulate photo-catalytic systems also have disadvantages given the separation of charge carriers is not as efficient as with a photo-electrode system, and there are difficulties associated with the effective separation of the stoichiometric mixture of oxygen and hydrogen to avoid the backward reaction.

1.4.4 Material requirements

Taking into account the photo-electrochemistry of water dissociation analyzed in the previous section, the photo-catalysts used for the photo-dissociation of water must satisfy several functional requirements with respect to semiconducting and electrochemical properties: (i) suitable solar visible-light absorption capacity with a band gap of around 2.0–2.2 eV and band edge potentials suitable for overall water splitting, (ii) capacity for separating photo-excited electrons from reactive holes, (iii) minimization of energy losses related to charge transport and recombination of photo-excited charges, (iv) chemical stability against corrosion and photo-corrosion in aqueous environments, (v) kinetically suitable electron transfer properties from photo-catalyst surface to water, and (vi) being easy to synthesize and cheap to produce.

1.4.5 Operating conditions affecting the photocatalytic hydrogen generation

Photocatalytic hydrogen generation by water splitting depends on following variables:

- Particle size and shape
- Morphology and structure of photo-catalyst
- Surface area of photo-catalyst
- Co-catalyst and sacrificial agents
- Retention time of water molecule on active site of photo-catalyst
- Mode of operation
- Operating temperature

Particle size and shape: Particle size and shape is the key feature of effective photo-catalytic material for hydrogen production. It mainly influences the band gap energy and surface area. On the other hand the manifestation of bulk recombination between photo generated charge carriers is promoted in large-sized photo-catalyst. So, the optimal particle size depends on composition. Small size particle exhibits broad section of highly crystalline phases. So, nano size particle is effective for photo-catalytic hydrogen generation. From another point of view powder sample (photo-catalyst) is difficult to handle for continuous mode of operation both vapor phase and

liquid phase. So, spherical beads of photo-catalyst with uniform size are required for the continuous hydrogen production from water. [7]

Morphology and Structure of photo-catalyst: The morphology and structure strongly depends on preparation method involved. Temperature and reagents used for the synthesis define particle size, shape, morphology and crystallinity. Eventual calcination phases after synthesis may also influence surface area and crystallinity. Theoretically, significant increases in photo-catalyst stability and crystallinity are amongst the primary targets of an effective calcination. However, in practice, beyond an optimum calcination temperature, lower photo-efficiencies due to agglomeration and sintering damage decreasing surface area, leading to phase transition is reported.

Surface area of photo-catalyst: The influence of the specific surface pattern of photo-catalysts on the hydrogen generation is quite controversial. A high specific area would increase not only the number of active catalytic sites, but also the number of superficial defect sites, which promote the recombination of free charge carriers. The deposition of selected noble metals on the surface of the photo-catalyst also decreases the electron-hole pair recombination. However, a high load of noble metal atoms favors the formation of surface metal clusters, which act as recombination centers. For that some computational techniques have been made for the analysis of optimum surface area design of suitable heterogeneous photo-catalyst in order to increase the rate of hydrogen generation.

Co-catalyst and sacrificial agents: Co-catalyst has an important role in production of photo-catalytic hydrogen generation. The amount and loading method of co-catalyst are crucial operating variables affecting hydrogen production. Co-catalyst nanoparticles with a uniform distribution can increase hydrogen production rate. However, excess loading may hinder radiation absorption and, in some cases promote photogenerated electron/hole recombination thus lowering process photoefficiency. So, an optimum co-catalyst load should be therefore identified.

Retention time of water molecule on active site of photo-catalyst: Photo-catalytic water splitting involves adsorption and surface reaction. As water splitting reaction is uphill reaction and follows slow kinetics, adsorption and high retention time of water molecule on active site of photo-catalyst is the key step for high yield of hydrogen production. Material should be designed

in such a way so that it provides larger retention time for the reaction. So photo-catalyst can be modified using water adsorbent material in an optimum way to increase hydrogen production.

Mode of operation: Till now usual photocatalytic water splitting reaction is operated in batch or semi-batch modes are reported. But for batch or semi-batch mode of operation industrial application is limited. Continuous mode of operation should be required for large scale of hydrogen production. On the other hand Gibbs free energy ($\Delta G^0=237.19$ kJ/mole) of liquid phase water splitting is larger than vapor phase water splitting. So, thermodynamically vapor phase water splitting is more favorable and will give better efficiency for hydrogen production. So, vapor phase with continuous mode is required to increase hydrogen production by water splitting reaction.

Effect of temperature: The effect of temperature on photocatalytic processes has to be taken into account due to different activation energy values for each physico-chemical step involved. Moderate increases in operating temperature enhance the hydrogen production rate. As a matter of fact, high temperatures promote charge carrier mobility, thus reducing the occurrence of photo-generated electron/hole recombination.

CHAPTER II

Literature review

Aim and Objectives

Literature review

2.1 Introduction

This chapter provides some information about the literatures surveyed and reviewed to perform the present investigation. Various studies involving Graphene based and adsorbent based nano-composite for hydrogen generation are conducted all over the world for the last few years. Here an attempt has been made to identify some of the main features, which may have some significant effect on performance and characterization of the catalysts and their effect on hydrogen production.

Title/Journal name/year/volume/pages	Author/s	Description
Highly efficient visible light driven photo-catalytic hydrogen production of CdS clauster-decorated Graphene nano-sheet. [JACS (2011) 133, 10878-10884]	Qin Li, Beidou Guo, Jiaguo Yu, Jingrun Ran, Baohong Zhang, Huijuan Yan, and Jian Ru Gong	A high efficiency hydrogen generation was achieved using Graphene nano sheet CdS-clauster as a visible light driven photo-catalyst. The material was prepared by solvothermal method n which GO served as a support material and cadmium acetate acts as CdS precursor. Activity of this catalyst is 1.12 mmol/h.
One dimensional CdS@MoS ₂ core shell nano-wires for boosted photo-catalytic hydrogen evolution under visible light. [Applied Catalysis B: Environmental]	Bin Hana, Siqu Liua, Nan Zhanga, Yi-Jun Xua, Zi-Rong Tanga	1D CdS@MoS ₂ core shell nano-wires are constructed by employing CdS nanowire as nanobuilding block via a facile hydrothermal strategy. The synergic interaction, stemming from large and

		<p>intimate coaxial interfacial interaction between MoS₂ thin shell and 1D CdS core, can efficiently retard the charge carrier recombination and the MoS₂ noble-metal-free co-catalyst enriches the active sites for hydrogen evolution from water. Comparison to pristine CdS nanowires, the resultant 1D core-shell CM composite exhibit distinctly enhanced visible light activity for the evolution of H₂.</p>
<p>Red-light-driven water splitting by Au(core) and CdS (shell) half-cut nanoegg with heteroepitaxial junction. [JACS, (2018), 140, 1251-1254]</p>	<p>Shin-ichi Naya, Takahiro Kume, Ryo Akashi, Musashi Fujishima, and Hiroaki Tada</p>	<p>The photo-catalytic activity depends on geometry and dimension, and the quality of junctions between the components. In this paper half-cut Au (core) and CdS (shell) nanoeggs as a new HNS plasmonic photo-catalyst was prepared for water splitting. HC-Au@CdS gives rise to continuous stoichiometric water splitting with high quantum yield on red light irradiation.</p>

<p>One pot synthesis of CdS-reduced Graphene oxide 3D composites with enhanced photo-catalytic properties.</p>	<p>Jiahong Wang, Shan Liang, Liang Ma, Sijing Ding, Xuefeng Yu, Li Zhou and Ququan Wang</p>	<p>In this paper nest like structure of CdS-rGO prepared by solvothermal technique. Ethylenediamine is used to reduce GO and control morphology of CdS. L-cystine was used as sulfide source, reducing source and linker between CdS and rGO. Compared with pristine CdS, prepared rGO-CdS catalyst showed enhanced light absorption, extended surface area, and facilitate separation of photogenerated charges. CdS-rGO has better catalytic activity than pristine CdS.</p>
<p>Synthesis of CdS quantum-dot sensitized TiO₂ nano-wires with high photo-catalytic activity for water splitting. [Journal of Photochemistry and Photobiology A: Chemistry 233 (2012) 65– 71]</p>	<p>Guosheng Wu, Min Tian, Aicheng Chen</p>	<p>On direct growth of uniform TiO₂ nanowires via facile thermal oxidation treatment of titanium substrate assisted by inorganic salts in presence of H₂O vapor. Synthesized TiO₂ nanowires were further modified with CdS quantum dots, which significantly increased the photocurrents. CdS quantum dot TiO₂ is visible light active catalyst.</p>

<p>Photo-catalytic activity of nano-sized cadmium sulfide synthesized by complex compound thermolysis</p> <p>[International Journal of Photoenergy Volume 2011, Article ID 762929]</p>	<p>Yingchun Yu, Youxian Ding, Shengli Zuo, and Jianjun Liu</p>	<p>The cubic CdS, hexagonal CdS, and their mixed phase were synthesized under the conditions of thiourea/Cd (S/Cd) molar ratios (0.5~3) of ≤ 1, ≥ 2, and 1.0~1.5, respectively. The grain size of CdS increases with the increased S/Cd ratio. The photocatalytic activity is in order of cubic > hexagonal > mixed phase, in which the cubic phase CdS has the best photocatalytic activity for RB degradation due to its strong adsorption, intense absorbance in visible region, and the smaller grain size.</p>
--	--	---

<p>MoS₂/CdS nanosheets-on nanorod heterostructure for highly efficient photocatalytic hydrogen generation under visible light irradiation.</p> <p>[ACS Appl. Mater. Interfaces 2016, 8, 15258–15266]</p>	<p>Xing-Liang Yin, Lei-Li Li, Wen-Jie Jiang, Yun Zhang, Xiang Zhang, Li-Jun Wan, and Jin-Song Hu</p>	<p>MoS₂/CdS nanohybrid as a noble-metal-free efficient visible light driven photocatalyst, which has a unique nanosheets-on nanorod heterostructure with partially crystalline MoS₂ nanosheets intimately but discretely growing on single-crystalline CdS nanorod. This heterostructure not only facilitates the charge separation and transfer owing to the formed heterojunction, shorter radial transfer path, and fewer defects in single crystalline nanorod, thus effectively reducing the charge recombination, but also provides plenty of active sites for hydrogen evolution reaction due to partially crystalline MoS₂ as well as enough room for extraction of hole.</p>
<p>Photo-catalytic hydrogen generation by CdSe/CdS nano particles.</p> <p>[Nano Lett. 2016, 16, 5347–5352]</p>	<p>Fen Qiu, Zhiji Han, Jeffrey J. Peterson, Michael Y. Odoi, Kelly</p>	<p>In this photo-catalytic activity was compared with various CdSe composites</p>

	L. Sowers, and Todd D. Krauss	like CdSe QDs, CdSe/CdS QDS, CdSe QRs and CdSe/CdS DIRs. CdSe has better efficient nano-catalyst among them for hydrogen generation. Size of the particle plays an important role in H ₂ generation.
Synthesis of CdS nano-particle using different sulfide ion precursors: Formation mechanism and photo-catalytic degradation of acid blue- 29. [Journal of Environmental Chemical Engineering 4 (2016) 808–817]	Nida Qutub, Bilal Masood Pirzada, Khalid Umar, Suhail Sabir	In this paper cadmium sulfide was prepared by using different sulfide ion precursors and studied photo-catalytic efficiency of differently synthesized cadmium sulfide photo-catalyst. The reactions were carried out by single pot chemical precipitation method under ambient condition. Average particles size were determined by TEM and XRD technique. An increase in photo-catalytic rate was observed by decreasing size of the particles.

2.1.1 Summary of literature review

After the extensive literature review it is observed that there are so many advantages and some of the research gap of this process. Process bottle necks and advantages of the process are discussed below.

2.1.2 Process bottle necks

- Photo-catalysts: Inability to utilize visible range
- High rate of recombination of photo generated electrons and holes
- Economically non-viable due to the use of expensive metals (e.g- Pt, Pd etc) as photo-catalyst and co-catalyst
- Thermodynamically water splitting reaction is a uphill reaction: Fast reverse reaction of formation of water from hydrogen and oxygen
- Low yield hydrogen production
- The usual operational mode of photo-catalytic hydrogen generation is in batch mode: Limitation in industrial application
- Slow kinetics due to low retention time of water molecule on active sites

2.2 Choice of Material

Choice of material and design of photo-catalyst is crucial step for photo-catalytic water splitting reaction. Material should be:

1. Visible light active
2. Narrow band gap semiconductor with low recombination rate
3. High porosity
4. Optimum surface area
5. Adsorbent based visible light active photo-catalyst
6. High photo-catalytic activity
7. High recyclability
8. High retention time

2.3 Role of adsorbent on photocatalytic water splitting

Slow kinetics is one of the major process bottlenecks for hydrogen generation by water splitting from both liquid and vapor phases. On the other hand thermodynamically backward reaction (formation reaction of water) is more favorable than forward reaction (splitting reaction). As photocatalytic water splitting reaction involves adsorption and heterogeneous surface catalyzed reaction, there are two controlling resistances:

- i) Adsorption controlling
- ii) Reaction controlling

Water splitting reaction follows slow kinetics so water molecule does not get sufficient retention time for the reaction with photo-catalyst. So, high retention time is very much needed for water splitting reaction so adsorption step is a crucial step for water splitting reaction. Novelty of our work is to incorporation of adsorbent into photo-catalyst. Adsorbent has main two roles in photocatalytic water splitting:

i) Adsorption of water molecule

ii) Provides high retention time for the reaction

Adsorbent is polymeric material containing $-OH$, $-NH_2$, $-COOH$ group so that water molecule can get attached by inter molecular hydrogen bonding. Various polymeric adsorbents are tested and selection is done based on the adsorption capacity.

2.4 Role of Graphene on photocatalytic water splitting

Graphene is a material composed of pure carbon atoms, arranged in a regular hexagon pattern. Graphene can be described as one-atom thick layer of graphite. It has drawn a lot of attention due to its great properties such as high optical transmittance, excellent electrical conductivity, high flexibility and larger theoretical surface area, and great chemical stability.

Graphene can be therefore utilized as:

i) Electron sink/ electron transporter: Graphene has high work function (4.42eV) and very high conductivity. Thus it can easily accept electrons from the conduction band of the photocatalysts semiconductors thereby checking the recombination of the photo generated electrons and hole and increasing the efficiency of the process.

ii) Co-catalyst: As reduction potential of Graphene is more negative than reduction potential of H^+/H_2 (-0.08 eV), it can be used as a co-catalyst to replace most commonly used costly noble metal co-catalyst (Pt).

iii) Photo-catalyst: Functionalized Graphene can be used to absorb solar spectra and can be used for solar water splitting as photo-catalyst. The conduction band minimum rGO is greater than that needed for hydrogen generation (-0.52 eV vs NHE, pH= 0) and the valence band maximum consists of mainly O 2p orbital that can be altered with varying degrees of reduction. [8]

iv) Photo-sensitizer: Graphene can be tuned to be used as a photosensitizer in light driven water splitting reactions. The electrons in photosensitizer are generated upon absorption of photon energy; these are accepted in CB of the photo-catalysts to produce hydrogen.

Thus the research objective is to develop a Graphene based semiconductor photo-catalyst that is able to absorb the visible spectra for the generation of hydrogen from water. The emphasis should be on the fabrication of an economical, efficient, reproducible, reusable photo-catalyst for the generation of hydrogen.

Content	Unit	values
Specific surface area	m ² /g	~2630
Electron mobility (at room temp.)	cm ² /V.s	~2.5×10 ⁵
Thermal conductivity	W/m.k	5.1×10 ³
C-C bond length in Single-layer graphene	nm	0.142

Fig-2.1 Properties of Graphene [9]

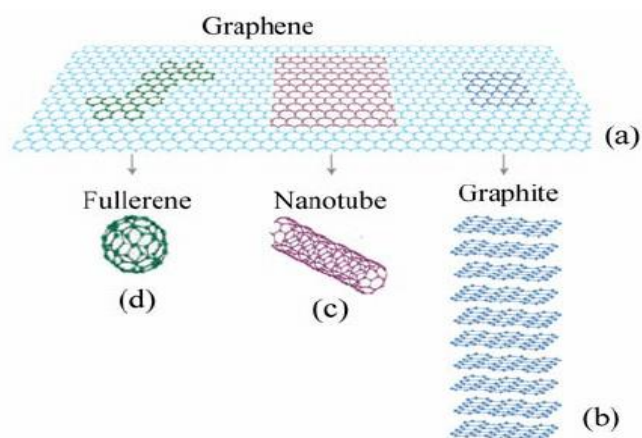


Fig-2.2 3D network of Graphene [10]

2.5 Research Gap

- Use of visible light active hybrid (water adsorbent-semiconductor) photo-catalyst for high rate of production of hydrogen
- Use of rGO based hybrid (water adsorbent-semiconductor) photo-catalyst for higher rate of production and higher quantum efficiency.

2.6 Aim and objective of the project work

2.6.1 The aim of the project work:

Design of rGO based water adsorbent-mediated visible light active hybrid photo-catalyst, rGO-CdS-Sodium Alginate, for enhanced hydrogen production from water.

2.6.1.1 Choice of CdS

As a visible light active photo-catalyst, cadmium sulfide (CdS) is one of the most representative materials. From UV-VIS spectroscopy we have seen that cadmium sulfide gives a peak within the visible range and band gap value is 2.42 eV. so, electron transfer from V.B to C.B is faster. On the other hand cadmium sulfide is prepared by very simply precipitation technique. From literature survey CdS has greater activity for HER (Hydrogen evolution reaction). Also cadmium sulfide has good recyclability. Although pristine CdS is not very effective for water-splitting but also by modification with Graphene, CdS acts as an effective photo-catalyst for water splitting reaction.

2.6.1.2 Choice of Sodium-alginate

Sodium alginate is a biopolymer containing –OH and –COOH with six membered cyclic ring. It has a very good moisture adsorbing capacity due to the presence of these functional groups. Water molecule is held by intermolecular hydrogen bonding with hydroxyl and acid groups. As pristine CdS is insoluble in water, so retention time of water molecule on active sites of CdS is very less. As sodium alginate is moisture adsorbing polymer, so it adsorbs water molecules on active sites of photo-catalyst when composite is formed and provides sufficient time for reaction. Thermodynamically water splitting reaction is not preferable ($\Delta G^0=237.18$ KJ/mole) so large retention time is the key factor for water splitting reaction to produce hydrogen.

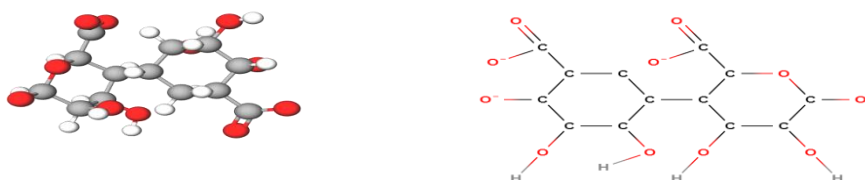


Fig-2.3 polymer network sodium-alginate

2.6.2 The specific objectives of the project

i) Synthesis of different visible light active photo-catalyst

- Synthesis of CdS
- Synthesis of CdS-Sodium alginate
- Synthesis of rGO-CdS-Sodium alginate

ii) Characterization of different photo-catalyst

- ❖ Identification of groups, crystallinity and Structural characterization: XRD, FTIR, SEM.
- ❖ Spectrophotometric characterization: UV-VIS spectroscopy: Determination of band gap

iii) Study of adsorption characteristics of the synthesized catalysts

iv) Generation of hydrogen using the synthesized photo-catalyst: Performance analysis

v) Comparative analysis of activity of different synthesized photo-catalysts

vi) Study of role of catalyst loading on the rate of production of hydrogen: determination of optimum catalyst loading

vii) Kinetic study of photocatalytic water splitting

viii) Study on Recyclability of the photo-catalyst

CHAPTER-III

Experimental work and Research Methodology

3.1 Synthesis of different photo-catalysts

3.1.1 Preparation of cadmium sulfide photo-catalyst:

Material required

1. Cadmium acetate (Sigma-Aldrich, 98% purity)
2. Thiourea (Sigma-Aldrich, 99% purity)
3. DI water

Synthesis procedure of cadmium sulfide:

5.56 gm. of cadmium acetate is taken in a beaker and 50 ml. of de-ionized water is added into it. Then it is stirred continuously for 1 hour to prepare 0.5 (M) solution of cadmium acetate. Then for the preparation of thiourea solution, 3.806 gm. of thiourea is taken in a beaker and 50 ml. of deionized water is poured into it and continuously stirred for 1 hour. Then prepared two solutions are mixed together in a large beaker and stirred for 10 hours at 80°C for the preparation of cadmium sulfide solution. Color change is the indication of CdS formation. Orange color solution of cadmium sulfide solution is obtained. Then this solution is filtered and dried at 70°C for 2-3 hours. Powder cadmium sulfide is prepared and kept in desiccator. [11]

Schematic diagram of synthesis procedure(Cadmium sulfide):

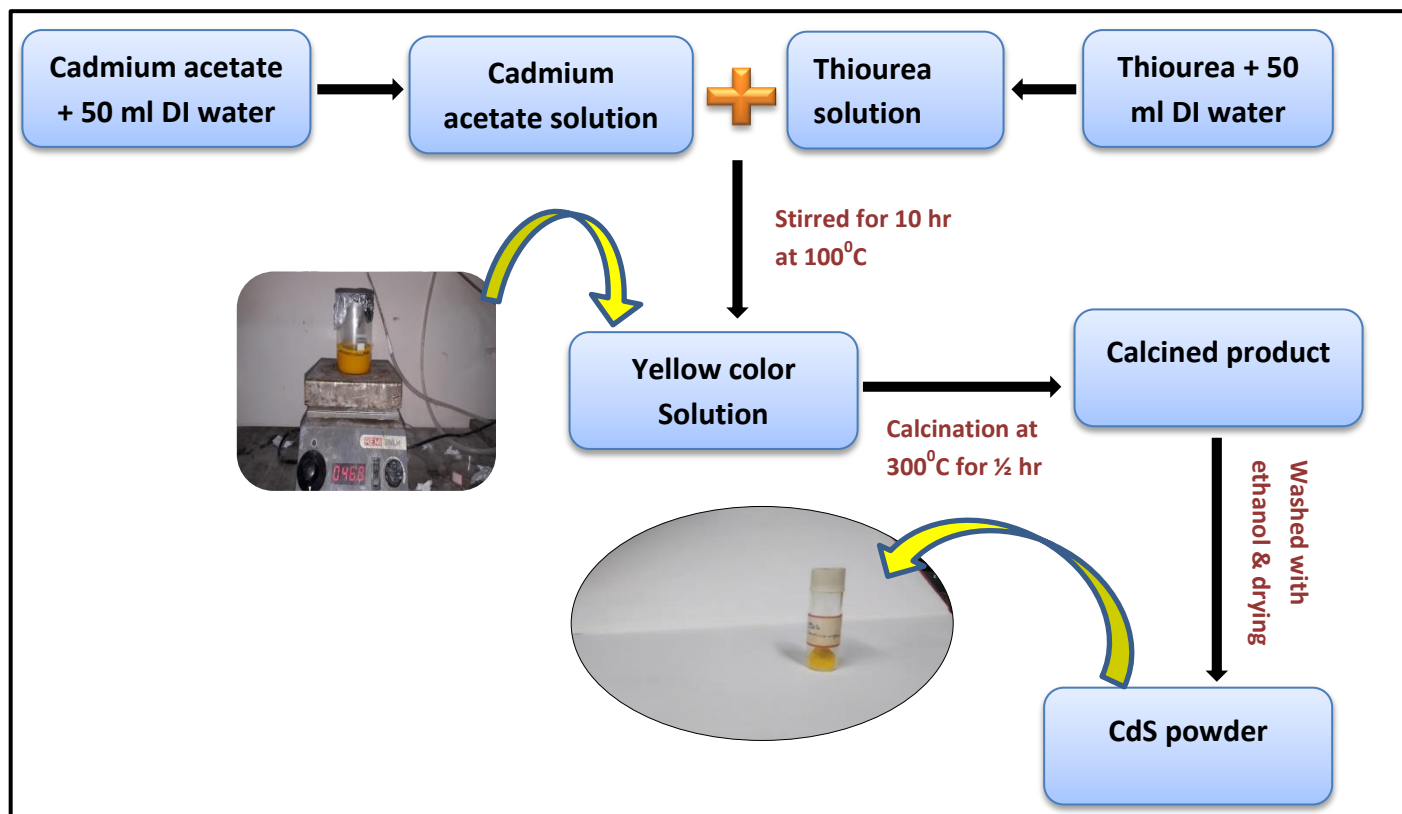


Fig-3.1 Process flow diagram of CdS synthesis

3.1.2 Preparation of CdS-Sodium alginate:

Materials required

1. Sodium-alginate powder (Sigma-Aldrich, 91% purity)
2. Cadmium- acetate (Sigma-Aldrich, 98% purity, M.W: 266.53 g/mol)
3. Thio-urea (Sigma-Aldrich, 99% purity)
4. De-ionized water

Synthesis procedure of sodium-alginate based cadmium sulfide:

1 gm. sodium-alginate powder is taken in beaker. Then 50ml. water is poured into this beaker and solution was stirred continuously for 2 hours at 70°C for the preparation of 2% (w/v) homogenous sodium-alginate solution. Then this prepared sodium-alginate solution is mixed with previously prepared cadmium sulfide solution and stirred at 50°C until the homogenous mixture is formed. Then this solution is taken into an autoclave and kept for 12 hours.

Schematic of synthesis procedure (Cadmium sulfide-sodium alginate):

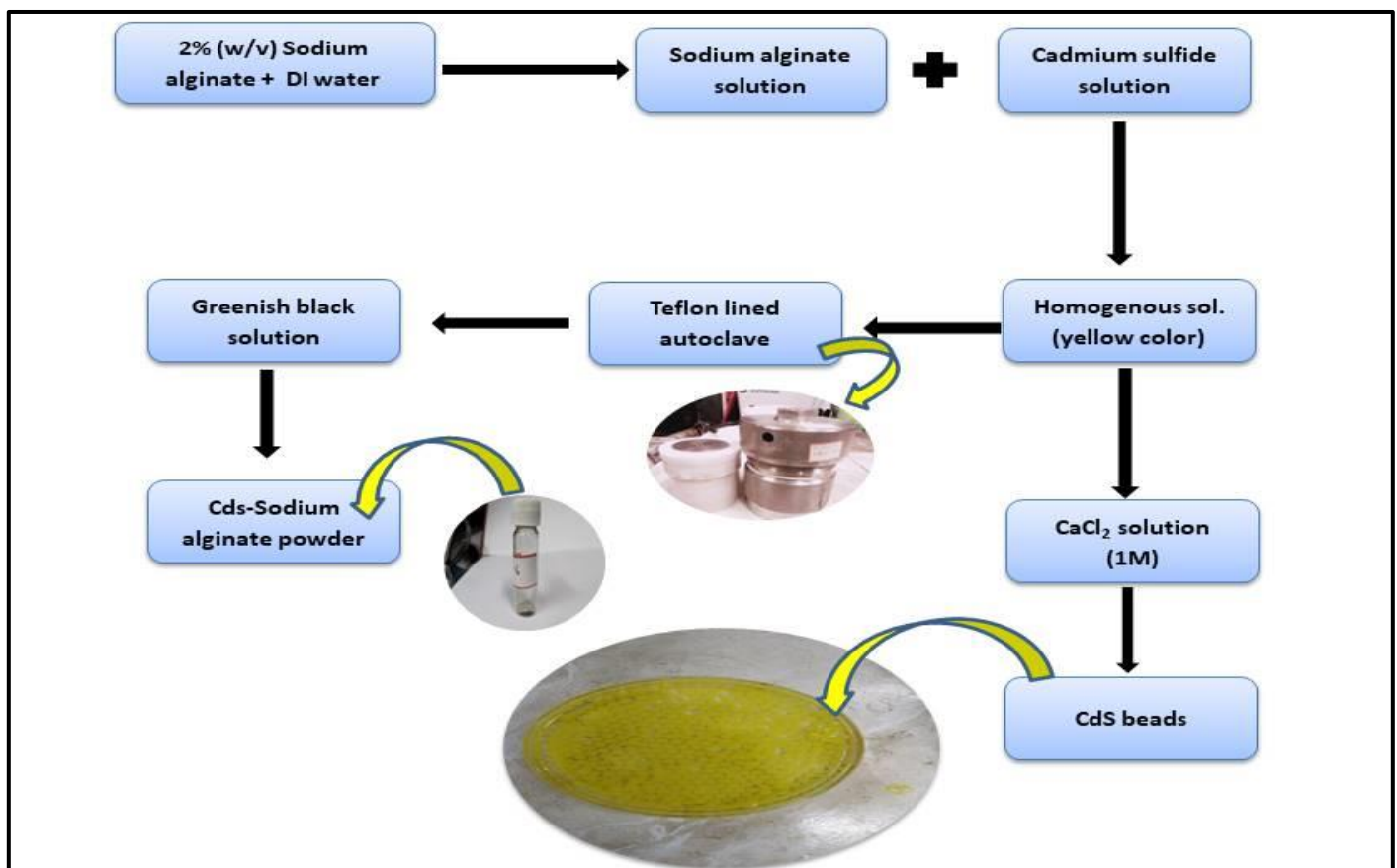


Fig-3.2 Process flow diagram of hybrid CdS-Sodium alginate

3.1.3 Preparation of Graphene-oxide:

Materials required:

1. Graphite flakes
2. Sulfuric acid (H_2SO_4)
3. Ortho-phosphoric acid (H_3PO_4)
4. Potassium permanganate (KMnO_4)
5. Hydrogen peroxide (H_2O_2)
6. Hydro-chloric acid (HCl)
7. Ethanol ($\text{C}_2\text{H}_5\text{OH}$)
8. Water (H_2O)

Synthesis procedure of Graphene-oxide:

There are many popular methods for the preparation of Graphene-oxide like

1. Hummer's method
2. Modified Hummer's method
3. Improved Hummer's method

Here we use improved modified Hummer's method for the synthesis of Graphene-oxide. [12]

Improved Hummer's method:

In the first step of improved method, a mixture containing H_2SO_4 360 ml. (98%) and H_3PO_4 40 ml. (88%) was prepared in a large beaker. Then 3.005 gm. graphite was added into the acid mixture and stirred continuously. 18.009gm. KMnO_4 was added slowly to the above mixture kept on an ice bath for temperature control.



Fig-3.3 KMnO_4



Fig-3.4 Graphite flakes



Fig-3.5 Stirring for 8 hrs.

The reaction mixture was stirred for 7-8 hours and the temperature maintained about 50⁰C-55⁰C during the stirring hour. After the stirring period the entire mixture is cooled to room temperature and 400 ml. ice & 3 ml. H₂O₂ were added to it for the termination of the reaction. After the cooling distilled water was added into the mixture and kept overnight.

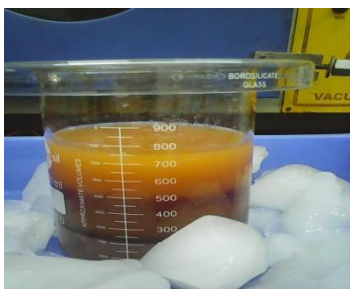


Fig-3.6 Termination step

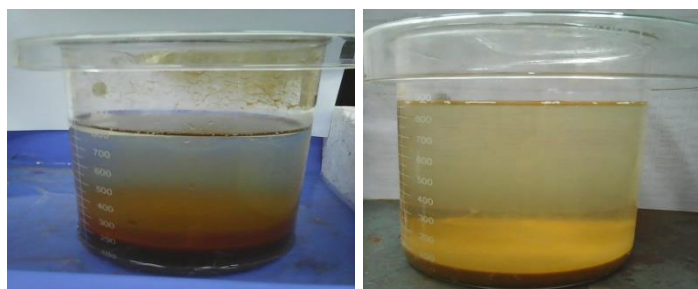


Fig-3.7 Different stages of washing

In day 2 after 12-14 hours a yellow color mixture was obtained and the mixture was washed in succession with 200 ml water, 200ml of 30% HCl and 200 ml ethanol and kept overnight. In 3rd day, 200 ml of ether was added and kept overnight for sedimentation to obtain a brownish yellow



Fig-3.8 Filtration



Fig-3.9 Drying

powder. In the 4th day 200 ml ether was added to the solution and filtered. Material is vacuum dried for 4-5 hours at room temperature and finally preserved in a vacuum desiccator for future use.

3.1.4 Preparation of rGO based CdS-Sodium-alginate (rGO-CdS-SA):

Materials required:

1. Cadmium acetate (Sigma-Aldrich, 98% purity)
2. Thio-urea (Sigma-Aldrich, 99% purity)
3. Sodium alginate powder (Sigma-Aldrich, 91% purity)
4. Graphene oxide
5. Urea (Sigma-Aldrich, 99% purity)
6. Water

Synthesis procedure of rGO based CdS- Sodium alginate photo-catalyst :

This composite is synthesized via hydrothermal procedure. Solution of Graphene Oxide (GO) is prepared by dispersing 0.2 % (w/v) GO in water and sonicated for about an hour. After that, this solution was added to the previously synthesized CdS –Sodium Alginate solution and stirred for about two hours. Reducing agent (urea) is added drop wise into the solution. This mixture was then sealed inside a 100 ml Teflon lined autoclave and kept at a temperature at 180⁰C for 20 hours. After that, the solution was washed several times and then dried in a vacuum oven at a temperature of about 80 °C and the dried sample was collected.

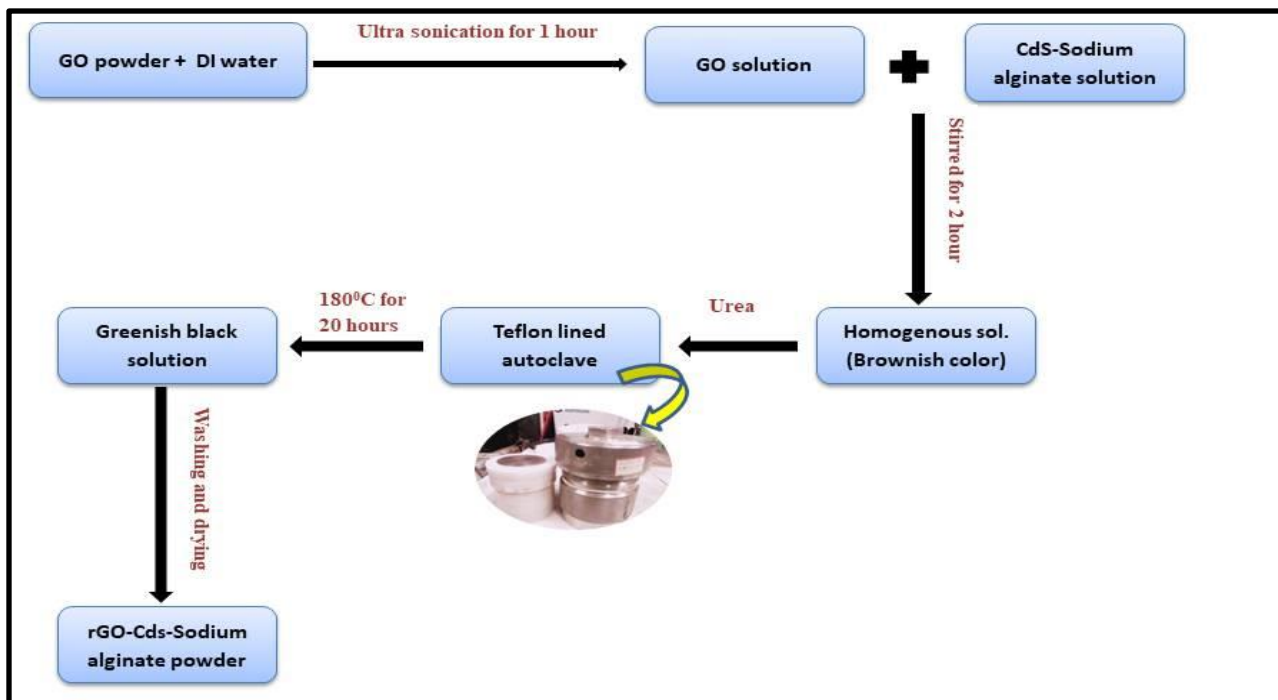


Fig-3.10 Process flow diagram of rGO-CdS-Sodium alginate

3.2 Characterization of synthesized catalyst

Three different synthesized photo-catalysts are characterized by SEM for structural determination, FTIR for group determination, XRD for crystallinity and UV-VIS spectroscopy for band gap calculation.

3.2.1 Structural characterization: scanning electron microscopy (SEM)

Sample preparation: Specimens are coated with a thin layer of 20 nm to 30 nm of conductive material of gold.

Operation and methodology: SEM uses an electron instead of a beam of light, which is directed towards the specimen under examination. An electron gun is located top of the device, shooting out a beam of highly concentrated electrons (15 kV) and SEM image is obtained. Image of the sample is shown in the next chapter.

Operating instrument: Hitachi S-3400 Scanning electron microscopy has been used to analyze the structural characterization of different synthesized catalysts.

3.2.2 Functional group determination: Fourier transformed infrared spectroscopy (FTIR)

Sample preparation: The powder sample and KBr must be ground in a mortar and pestle to reduce particle size to less than 5 μm in diameter. Then pellet formation of the sample is done under high pressure and tested by FTIR instrument.

Operation and methodology: The sample absorbance of the infrared light's energy at various wave lengths is measured to determine the material's molecular composition and structure. The frequency range is measured as wave number over the range of 4000 cm^{-1} to 400 cm^{-1} . Percentage transmittance vs wave number is plotted and analyzed the peak. Analysis is shown in the next chapter.

Operating instrument: Perkin Elmer Spectrum-2 is used for FTIR analysis of different synthesized photo-catalyst.

3.2.3 Crystallinity of samples: X-ray diffraction (XRD)

Sample preparation: Powder XRD is carried using a pinch of sample.

Operation and methodology: X-ray falls on the sample and reflected x-ray is detected by X-ray detector. Governing principle for XRD is Bragg's law ($n\lambda=2d\sin\theta$). Different peaks are obtained at various 2θ angles with various intensities. Then intensity vs. 2θ is plotted and peaks are analyzed using JCPDS library and literature review for crystal plane. Analysis of XRD is shown in the next chapter.

Operation instruments: Rigaku, Ultima III Diffractometer is used for XRD analysis.

3.2.4 Band gap calculation: UV-VIS spectroscopy

Sample preparation: Pinch of powder sample is dispersed into water by ultra-sonication for 15 min. and taken into quartz cuvette for the UV-VIS spectroscopy.

Operation and methodology: UV-VIS spectroscopy follows Lambert's Beer law. Two cells are used for this analysis one is reference cell (water) and another is sample cell (aqueous solution of catalyst). Monochromatic beam of light is passed through the sample and reference cell both and gives the absorbance vs wavelength plot.

Band gap calculation: For optical band gap can be measure by empirical relation known as Tauc formula: $\alpha hv = A(hv - E_g)^n$ (3.1)

Where, hv = Photon energy

α = Absorption co-efficient

A = Constant

n = Constant depending upon the transition

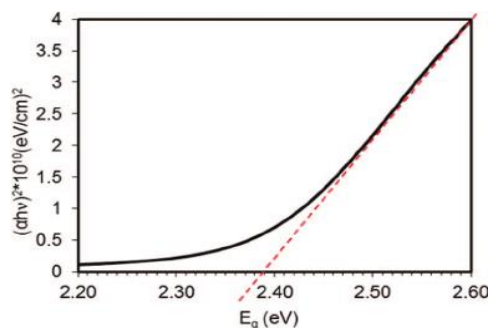


Fig-3.11 Tauc plot [13]

Here, $A=1$ and $n=1/2$ so, the formula can be written as $(\alpha hv)^2 = (hv - E_g)$

$hv = hc/\lambda = 1240/\lambda$

A graph is plotted between $(\alpha hv)^2$ as an ordinate and hv as abscissa. The extrapolation of straight line to $(\alpha hv)^2 = 0$ axis (Tauc plot) helps in obtaining the value of band gap.

Operational instrument: Perkin Elmer 365 UV-VIS spectroscopy is used for this analysis.

3.3. Experimental methodology

3.3.1 Study on adsorption characteristics of different water adsorbents: Generation of Adsorption Isobar

Different water adsorbent polymers are used for studying adsorption characteristics. Here adsorption study is carried out in a humidification chamber at different temperatures. Chitosan and sodium alginate are used for this experiment. 0.5 gm of each polymer is taken in a Petri-dish and kept inside humidification chamber for 12 hours. After 12 hours the final weight is taken. The increase in weight is the amount of water adsorbed. Amount of adsorption is examined at different temperatures with a fixed relative humidity (90%). Among two polymers sodium alginate has better adsorption capacity.

3.3.2 Generation of hydrogen using the synthesized photo-catalyst: Performance

Process description: Photo-catalytic hydrogen generation

Generation of hydrogen from liquid phase water by photo-catalytic water splitting is occurred in the following fashion:

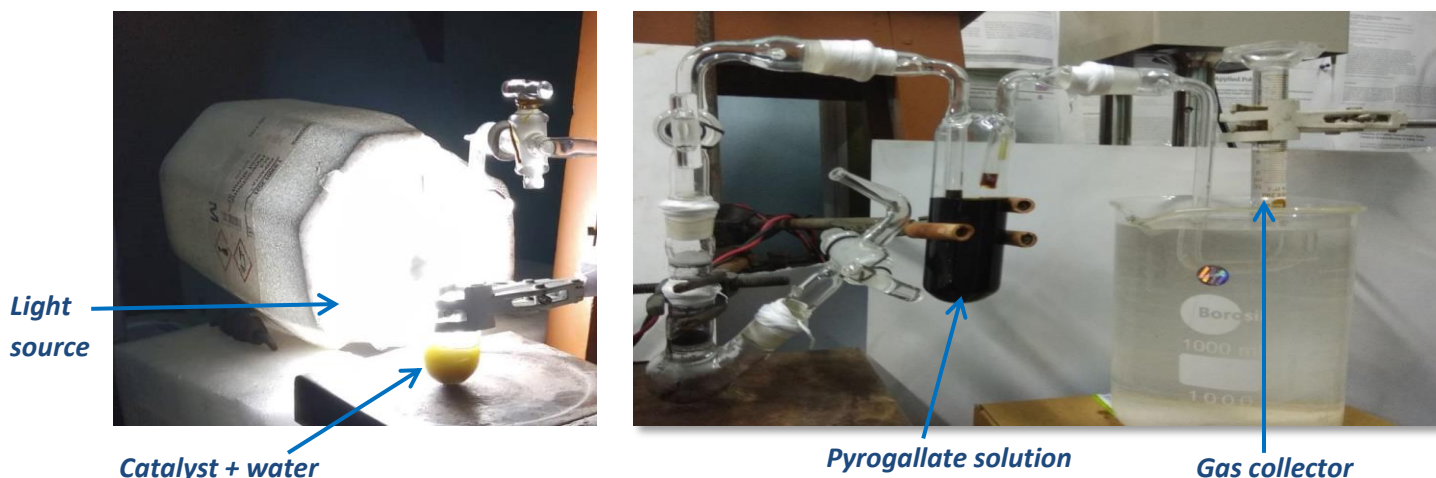
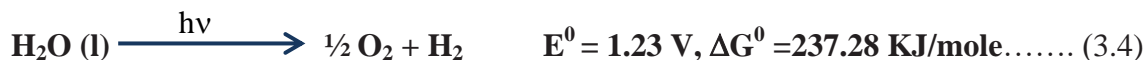
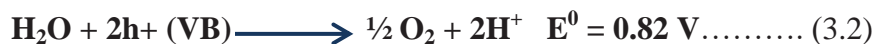


Fig-3.12 Experimental setup

The above laboratory scale photo-reactor (volume of the reaction vessel is 30 ml.) setup is used for the performance analysis of different photo-catalysts. This reactor is operated in semi batch mode of operation. There are several components of the reactor:

- i) Visible light source (100 watt lamp)
- ii) Reaction vessel
- iii) Gas outlet
- iv) Oxygen trap
- v) Gas collector

The setup consists of a basic light bulb (100 watt) arrangement as a light source. A small 25 ml pyrex (Borosil) volumetric flask is used as a reactor vessel. It is fitted with a stand and clamp. The photo-catalyst is added to the water present in the flask. Sacrificial agent may be added. The volume of water taken is 15 ml. The different amount of photo-catalyst is used for performance study. The solution is continuously stirred by magnetic stirring. The photograph of the reactor setup is shown above. After some time, gradual bubble formation is observed. The evolving gas is collected by displacing water in an inverted water filled with graduated measuring cylinder (10 ml) kept in a beaker filled with water. Before that the gas is passed through oxygen trapping setup containing alkaline pyrogallate solution. The time and the volume of gas generated are noted down and collected as a data sheet.

Parameter of the reaction:

Phase	Liquid
Volume of water	15 ml.
Light intensity	Above 20Klux
Temperature	Room temperature
Stirring speed	600 rpm.

Performance analysis using pristine CdS, CdS-Sodium Alginate and rGO-CdS-Sodium Alginate:

The performance analysis of the photocatalytic water splitting is studied primarily using pristine CdS as a base study. CdS is a well-known photo-catalyst with a bandgap of 2.4 eV and is able to absorb the visible spectrum of light. 10 mg of CdS is first dissolved in 15 ml of distilled water.

Few drops of methanol are added. The photoreactor is then illuminated with a 100 W LED lamp. The evolved gas is then passed through an alkaline solution of pyrogallol and is collected by the downward displacement of water. After that the nano-hybrid CdS-Sodium Alginate is used for comparative study. Equal loading with CdS-Sodium Alginate is used for comparison. The data is collected over the course of time and is noted down. Then, same loading with rGO-CdS-Sodium alginate is added and the result is plotted.

3.4 Comparative study of photocatalytic activity of different synthesized catalyst

Effect of different synthesized photo-catalyst for hydrogen generation is examined by taking the 10 mg of each catalyst separately in a laboratory scale photo reactor and the same procedure is carried out (Discussed in previous section) for each time with similar operational parameter. The comparative analysis is done among three synthesized catalysts. From the experimental data it can be seen that the rGO based hybrid CdS- Sodium Alginate catalyst gives the better performance compared to pristine CdS and hybrid CdS-Sodium Alginate for photocatalytic hydrogen generation under visible light condition.

3.5 Study on change in catalyst loading for optimum photocatalytic activity

To determine the effect of the catalyst loading for optimum photocatalytic activity, several batches of experiment is conducted by varying the amount of catalyst in the range of 10 mg to 40 mg. The effect of catalyst loading on photo-catalytic water splitting is studied using the amount of catalyst (rGO-CdS-Sodium alginate) of 10 mg, 20 mg, 30mg and 40 mg with similar operational parameter. With increase in catalyst loading hydrogen generation increases and reaches an optimum point. In this experiment 40 mg. of catalyst loading is the optimum loading for 15 ml of water.

3.6 Study of effect on photocatalytic water splitting upon catalyst recycling

Recyclability is an important aspect for heterogeneous photocatalytic water splitting. First of all freshly prepared catalyst is used for photocatalytic hydrogen generation and data is collected. Then 7 days, 15 days and 30 days later same procedure is carried out to measure photo-catalytic activity of photo-catalyst by using same catalyst. From the result it can be seen that

photocatalytic activity of regenerated photo-catalyst decays with time. The experiment is carried out in a same manner that is discussed in the performance analysis section.

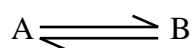
3.7 Kinetic study of photocatalytic water splitting

Kinetic study is important for understanding the behavior of a reaction. Kinetic study is analyzed by following two methods.

i) Integral analysis

ii) Differential analysis

Here differential analysis is done. Water splitting reaction is a reversible reaction with surface adsorption. So we consider the Langmuir-Hinshelwood kinetics [14] for the analysis.



$$-r_A = K_1 C_A / (1 + K_2 C_A) \dots\dots\dots (3.5)$$

$$1/(-r_A) = (1/K_1 C_A) + (K_2/K_1) \dots\dots\dots (3.6)$$

Where, K_1 = Forward rate constant

K_2 = Backward rate constant

C_A = Concentration of the reactant

If $(1/-r_A)$ vs $(1/C_A)$ are plotted and reasonably good straight line obtained, then rate equation is said to be satisfactorily fit the L-H kinetics model. [15]

L-H kinetics:

L-H kinetic model can be applied for heterogeneous surface catalyzed reaction & can be considered as ‘**standard**’. The same idea is applied in our modeling purpose. A simple heterogeneous catalyzed reaction involves series of consecutive steps

i) Adsorption

ii) Surface reaction

iii) Desorption

The one of which is substantially slower than the others. The slow step, generally chemical reaction of adsorbed molecules on the catalyst surface is described by a kinetic equation is known as L-H model that is given above.

Kinetic study is done by following steps (Methodology):

- 1) First plot the experimental data of C_A vs t and draw smooth curve to represent the data
- 2) Fit this data with a mathematical equation
- 3) Differentiate this equation at different time value to get the rate of the reaction ($-dC_A/dt$)
- 4) Plot $(1/-r_A)$ vs $1/C_A$ and gives a straight line and it is reasonably fit with the L-H model.

This is analyzed by the help of MATLAB and Origin software.

CHAPTER-V

Result and discussion

4.1 Result and discussion

Characterization of photo-catalyst

Three different photo-catalysts are synthesized via several routes such as Chemical impregnation- method, hydrothermal synthesis and precipitation technique respectively. In this section photo-catalyst are characterized using UV-Vis spectroscopy, XRD, FTIR and SEM analysis reveal noble adsorbent based photo-catalyst with excellent catalytic ability.

4.1.1 Morphological Characterization: Scanning electron microscopy (SEM)

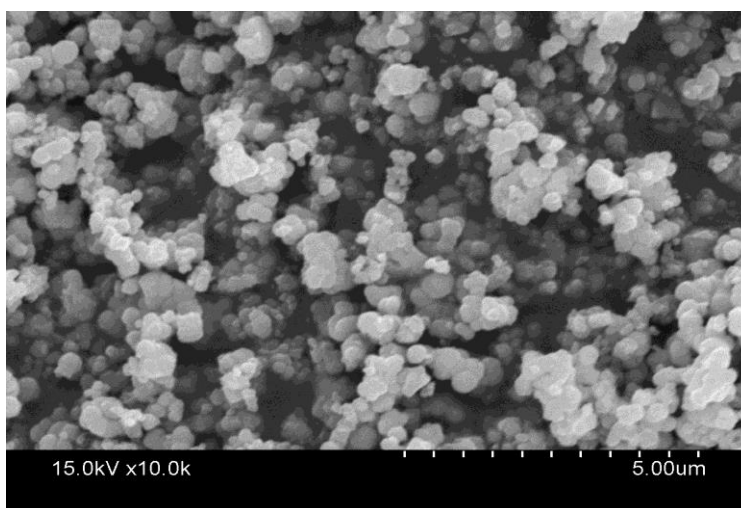


Fig-4.1 Representative SEM images of CdS nanocatalyst

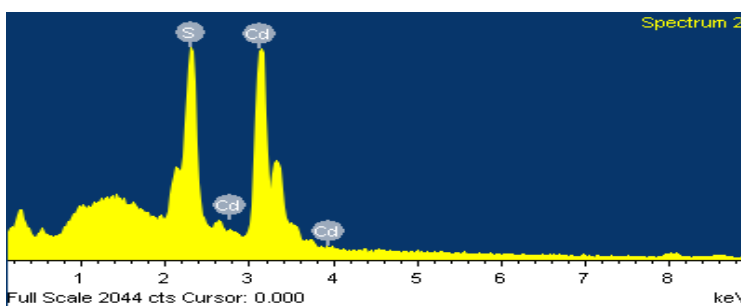


Fig-4.2 EDAX spectrum of CdS nanocatalyst

SEM image of Cadmium sulphide (CdS) nanoparticles at a scale bar of 2.00 μm can be seen in the adjacent picture. The image is obtained using Hitachi S-3400 at an accelerating voltage of 15.0 kV. Homogenously distributed nano-flower like structures of CdS can be seen from the SEM image. [16]

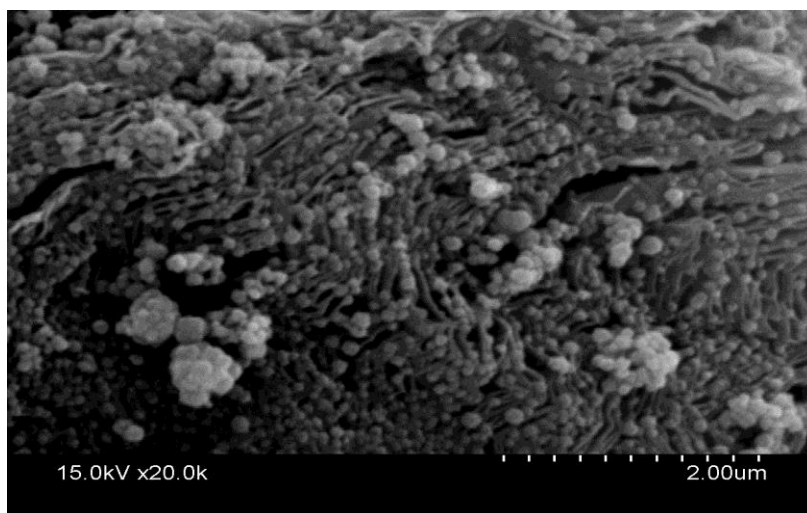


Fig-4.3 Representative SEM images of hybrid CdS-Sodium alginate nanocatalyst

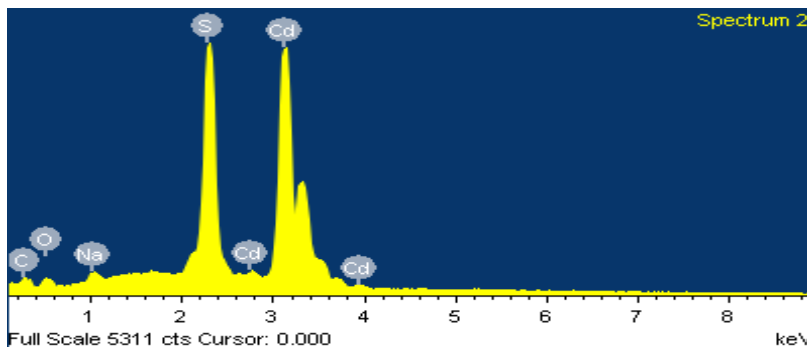


Fig-4.4 EDAX spectrum of hybrid CdS-Sodium alginate nano-catalyst

SEM image of Cadmium sulphide (CdS) /Sodium Alginate nanoparticles at a scale bar of 2.00 μm can be seen in the adjacent picture. The image is obtained using Hitachi S-3400 at an accelerating voltage of 15.0 kV. Nano-fibrils of Sodium Alginate can be seen interspersed with nano-flowers of CdS from the SEM image. [17]

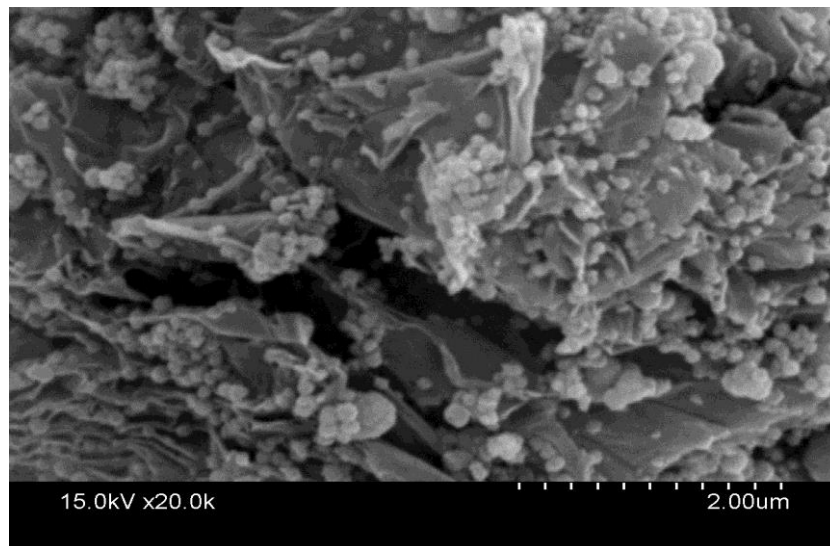


Fig-4.5 Representative SEM images of rGO-CdS-Sodium alginate photo-catalyst

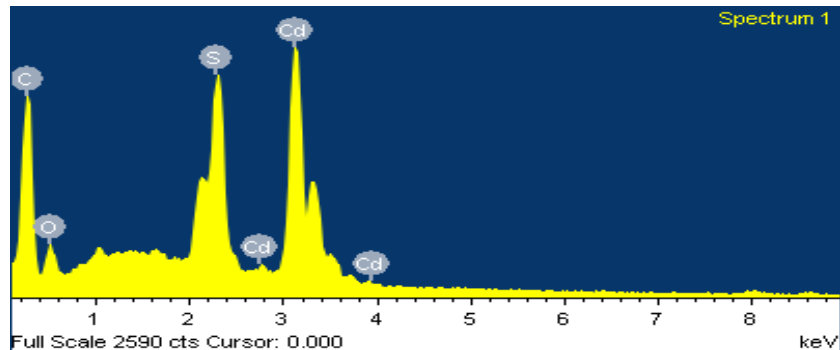


Fig-4.6 EDAX spectrum of rGO-CdS-Sodium alginate photo-catalyst

SEM image of Cadmium sulphide (CdS) /Sodium Alginate nanoparticles at a scale bar of 2.00 µm can be seen in the adjacent picture. The image is obtained using Hitachi S-3400 at an accelerating voltage of 15.0 kV. Nano-fibrils of Sodium Alginate can be seen interspersed with nano-flowers of CdS distributed on the crumpled up sheets of Graphene. The crumpled up structure of Graphene might be due the effect of exfoliation and the process of restacking. [18]

4.1.2 Characterization for functional group determination: Fourier transformed infrared spectroscopy

Fig-4.7 shows that FTIR spectra of CdS, CdS-Sodium alginate and rGO-CdS-Sodium alginate respectively. In spectrum Fig-4.7, a strong and broad absorption is observed at 3466.35 cm^{-1} due to O-H stretching vibration. The C=O stretching of COOH groups situated at edges of sodium alginate is observed at 1729 cm^{-1} . At 872.65 cm^{-1} corresponds to Cd-S stretching. [19] Bands at 1564 cm^{-1} correspond to N-H bending.

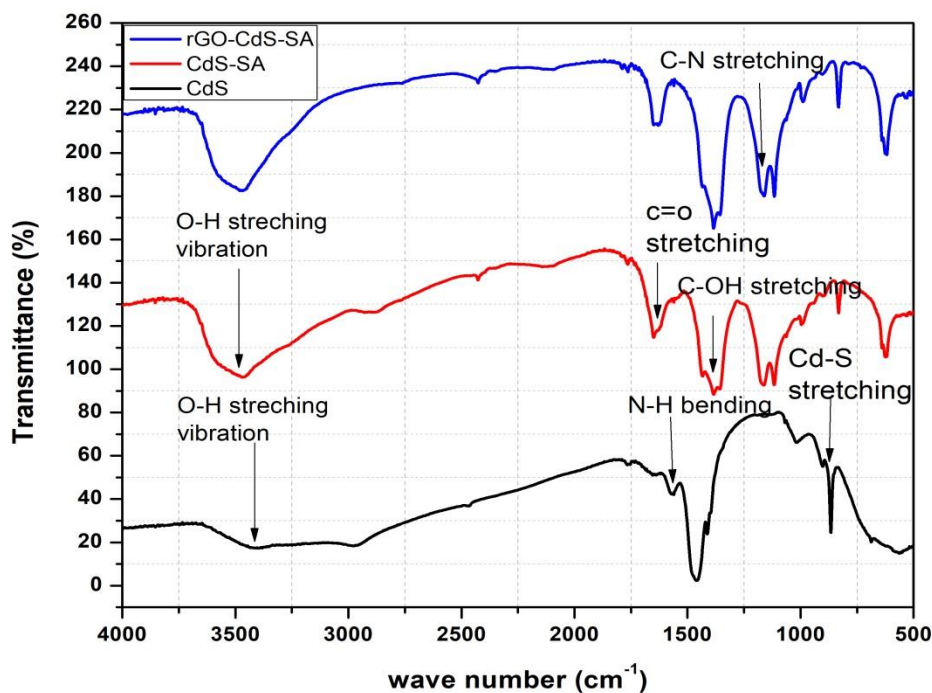


Fig-4.7 FTIR images of CdS/ CdS-Sodium alginate and rGO-CdS-Sodium alginate photocatalyst

4.1.3 Characterization for crystallinity: X-ray diffraction (XRD)

Fig-4.8 shows that the XRD pattern of CdS, CdS-Sodium alginate and rGO-CdS-Sodium alginate respectively. XRD pattern of CdS can be assigned to cubic phase of CdS (β phase). [19] The three main diffraction peaks are corresponding to (111), (220) and (311) planes respectively. On addition of sodium alginate and reduced Graphene oxide widening of peak can be seen when compared with pristine CdS.

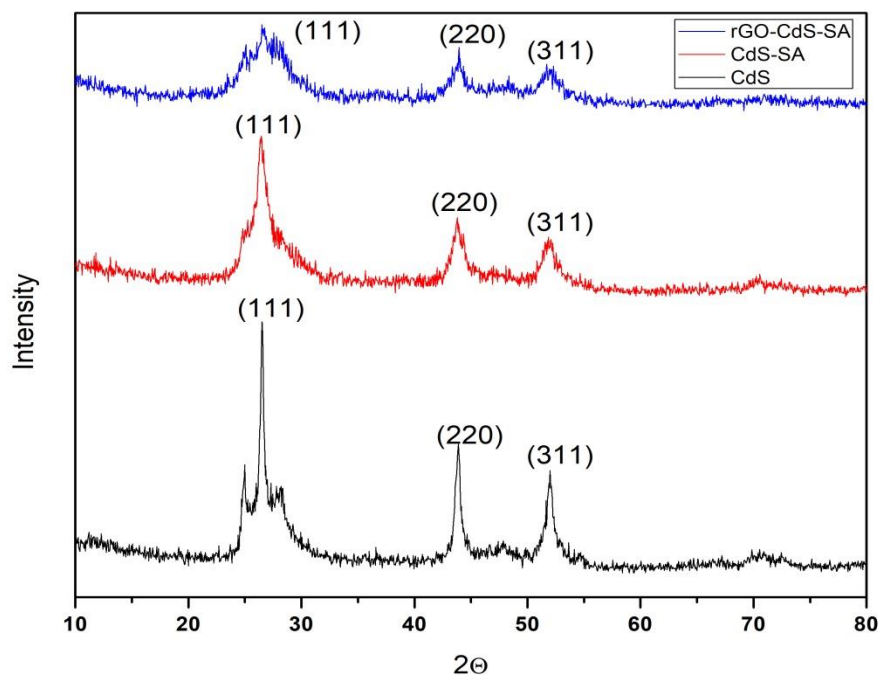


Fig-4.8 The XRD pattern of CdS/ hybrid CdS-Sodium alginate and rGO-CdS-Sodium alginate

Grain size:

Mean grain size of the deposited CdS is calculated using Scherer formula [20]

$$D = K\lambda/\beta\cos\theta \dots\dots\dots (4.1)$$

Where, D = Size of the crystallites (nm)

K = 0.9 (Scherer constant)

λ = 0.15406 nm (wavelength)

β = FWHM (radians)

θ = Peak positions (radians)

For calculation β is observed by zooming the peak position using origin software. The calculated average grain size of CdS comes out to be nearly 9nm to 11nm.

Sample	Average size (nm)
CdS	10.08432088
rGO-CdS-SA	9.304871694
CdS-SA	10.909906799

4.1.4 Spectrophotometric characterization: UV-VIS spectroscopy: Band gap calculation

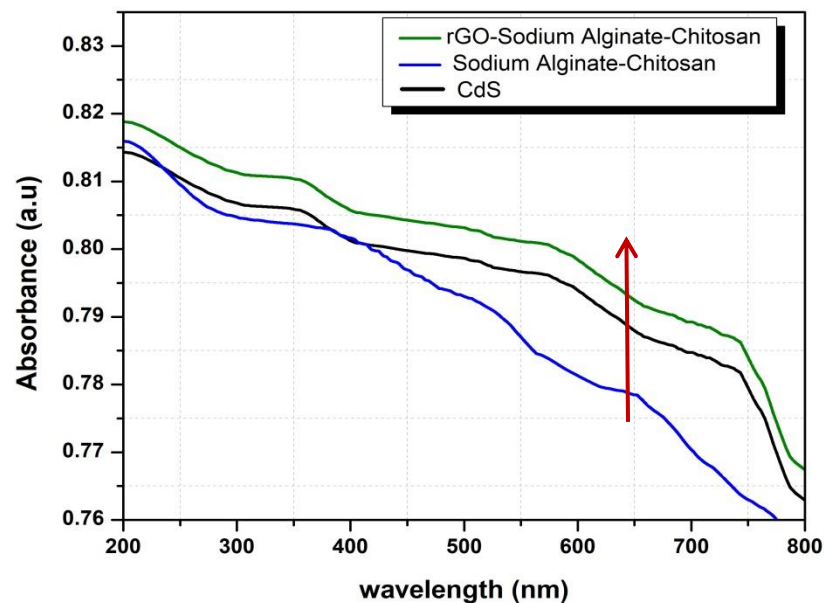


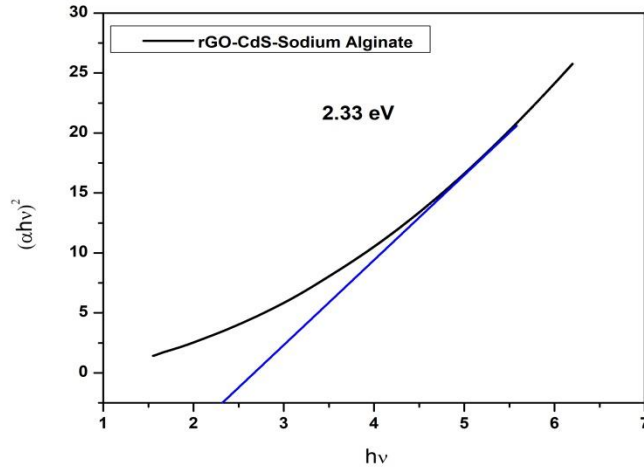
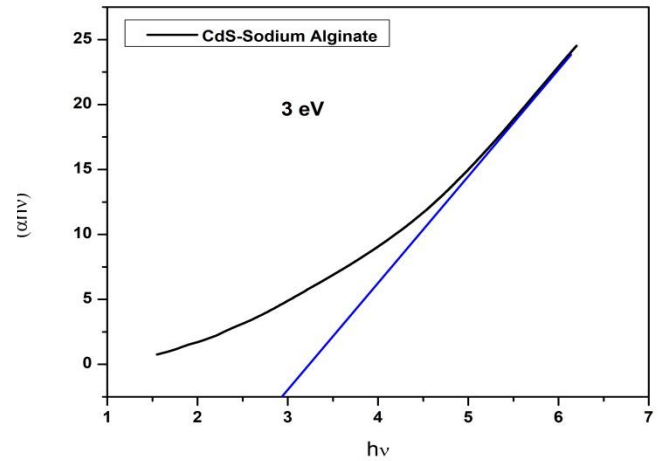
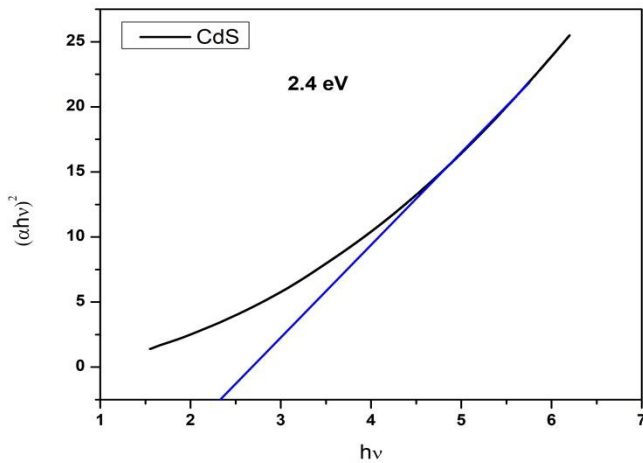
Fig-4.9 UV-VIS spectroscopy of different synthesized catalyst: Pristine CdS/ hybrid CdS-Sodium alginate and rGO-CdS-Sodium alginate

From the Fig-4.9 it can be observed that peak is obtained at 407.23 nm, 353.59 nm. and 390 nm. for pristine CdS, hybrid CdS-Sodium alginate and rGO-CdS-Sodium alginate respectively. [19]

There is an enhanced absorbance by the addition of Graphene. From the result, we can infer that g reduced Graphene oxide based water adsorbent mediated photo-catalyst (rGO-CdS-Sodium alginate) is effective for visible-light response for water splitting.

Band gap:

Calculated band gap is shown in the table below



Name of the photo-catalyst	Band gap energy
Pristine CdS	2.4 Ev
Hybrid CdS-Sodium alginate	3.0 Ev
rGO-CdS-Sodium alginate	2.33 Ev

4.2 Experimental result

The noble adsorbent (sodium alginate) based photo-catalyst preparation and characterization are discussed in earlier chapter. In this chapter, the catalytic performance and adsorption study is investigated by water splitting reaction using laboratory scale photo-reactor setup.

4.2.1 Study on adsorption characteristics of different water adsorbents: Generation of Adsorption Isotherm

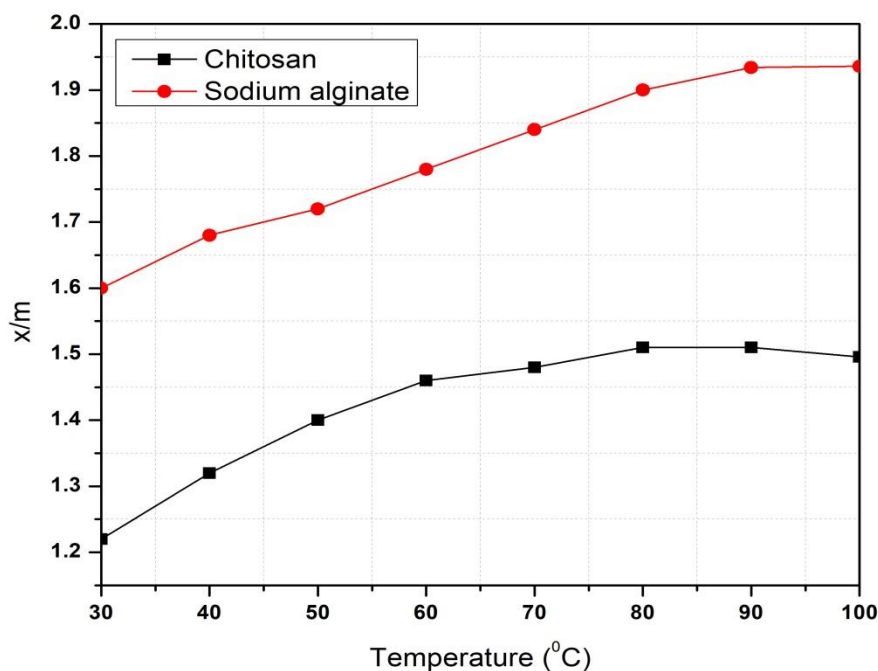


Fig-4.10 Moisture adsorbed/mass of adsorbent (x/m) vs temperature plot

From the graph it can be seen that with increasing temperature adsorption increases and reaches maximum value at higher temperature. [20] The initial increasing extent of adsorption with increasing temperature confirms chemisorption; the heat supplied acts as the activation energy required in chemisorption. Maximum moisture adsorbed/ unit mass of adsorbent (x/m) by chitosan and sodium alginate polymer is 1.496 and 1.936 respectively at 90% relative humidity. Therefore between two adsorbents, sodium alginate has better moisture adsorbing capacity and

provides larger retention time for photocatalytic water splitting reaction. So sodium alginate is utilized in this work as an adsorbent.

4.2.2 Performance study of different photo-catalyst

Base case study: Performance analysis using pristine CdS

Table shows the moles of hydrogen generation with respect to time. With increasing time hydrogen generation increases under the visible spectrum of light using pristine CdS. Maximum hydrogen generated during 3 hours of operation is 95.08 μ moles.

Time (min.)	Moles of hydrogen generated (μ moles)
0	0
30	5.8
60	12.48
90	26.34
120	46.1
150	76.34
180	95.08

Graphical presentation: performance analysis using pristine CdS (10 mg. catalyst loading)

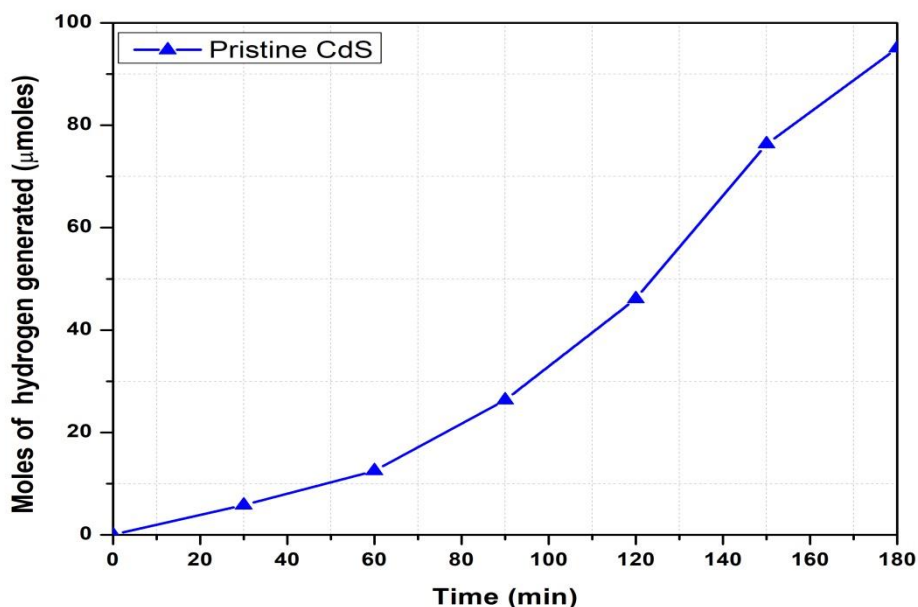


Fig-4.11 Moles of hydrogen generated vs time plot using Pristine CdS with 10 mg of catalyst loading

Performance analysis using CdS-Sodium alginate:

Table shows that using Sodium alginate based CdS composite; hydrogen generation is enhanced from 95.08 μmoles to 120.63 μmoles . So it can be concluded that adsorption has an important role in photocatalytic water splitting to produce hydrogen. Because of the presence of sodium alginate it provides larger retention time of water to react with active sites of photo-catalyst and hydrogen generation is increased 20% at same operational parameter.

Time (min.)	Moles of hydrogen generated (μmoles)
0	0
30	11.9
60	26.78
90	41.66
120	53.52
150	71.42
180	120.63

Graphical presentation: Performance analysis using CdS-Sodium alginate (10 mg.)

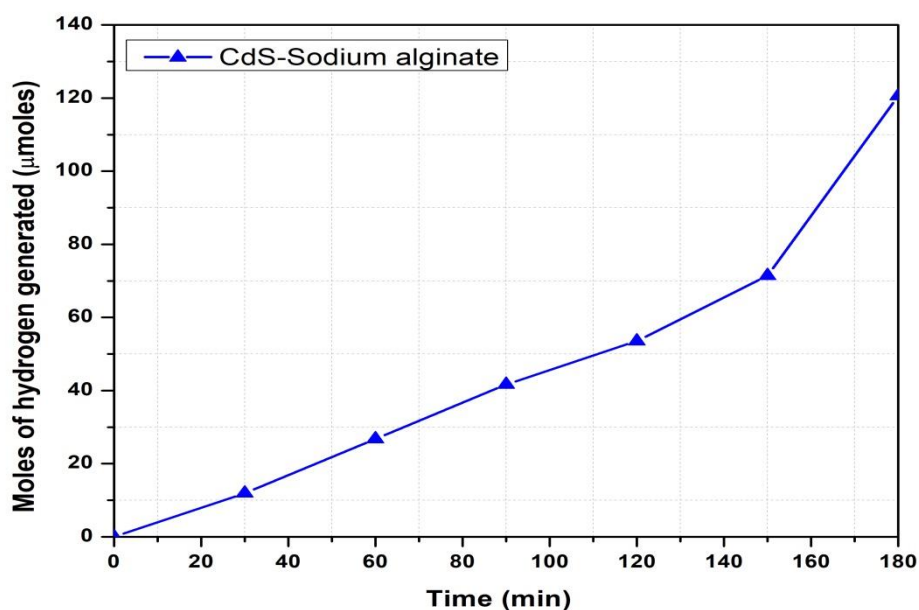


Fig-4.12 Moles of hydrogen generated vs time plot using hybrid CdS-Sodium alginate with 10 mg of catalyst loading

Performance analysis using rGO-CdS-Sodium alginate:

Using reduced Graphene oxide along with CdS-Sodium alginate, photo-catalytic hydrogen generation is further increased from 120.63 μmoles to 146.64 μmoles . Graphene has an important role in photocatalytic hydrogen generation that is discussed earlier in chapter-4. In this case hydrogen generation is increased 17% with respect to CdS-Sodium alginate and 35% with respect to pristine CdS. This is graphically shown in the figure below.

Time (min.)	Moles of hydrogen generated (μmoles)
0	0
30	20.5
60	38.01
90	70.5
120	98.42
150	123.1
180	146.64

Graphical presentation: Performance analysis using rGO-CdS-Sodium alginate (10 mg.)

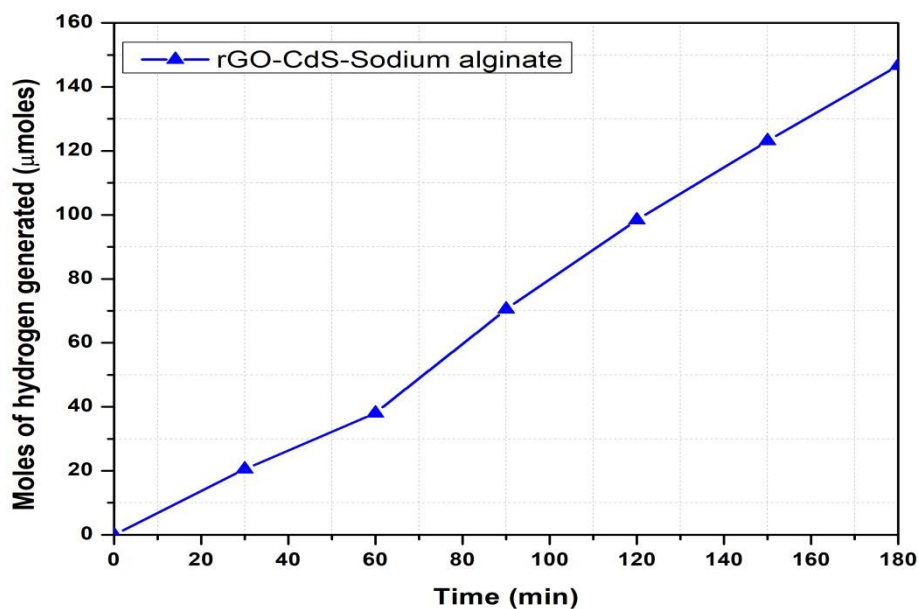


Fig-4.13 Moles of hydrogen generated vs time plot using rGO-CdS-Sodium alginate with 10 mg of catalyst loading

4.2.3 Comparative analysis of different catalyst

Catalyst name	Catalyst loading	Total moles of hydrogen (μmoles)
Pristine CdS	10 mg.	95.08
CdS-Sodium alginate	10 mg.	120.63
rGO-CdS-Sodium alginate	10 mg.	146.64

For three hours of operation 95.08 μmole , 120.63 μmole and 146.64 μmoles hydrogen are generated using pristine CdS, hybrid CdS-Sodium alginate and rGO-CdS-Sodium alginate respectively. Pristine CdS is less effective than others.

Role of sodium alginate: The presence of sodium alginate, CdS gives better performance because sodium alginate is a moisture adsorbing polymer so retention time of water molecule on reactive sites increases for the reaction without any co-catalyst. Addition of sodium alginate into pristine CdS increases the band gap value of hybrid catalyst from 2.4 eV to 3 eV, so rate of recombination decreases and facilitates the hydrogen generation.

Role of reduced Graphene oxide: Further addition of reduced Graphene oxide on CdS-Sodium alginate composite gives better result than CdS-Sodium alginate. Because of the presence of Graphene sheet it provides larger surface area and facilitates the transport of electron due to decrease of band gap value to 2.33 e.V as well as Graphene itself acts as photo-catalyst. Therefore hydrogen generation increases further.

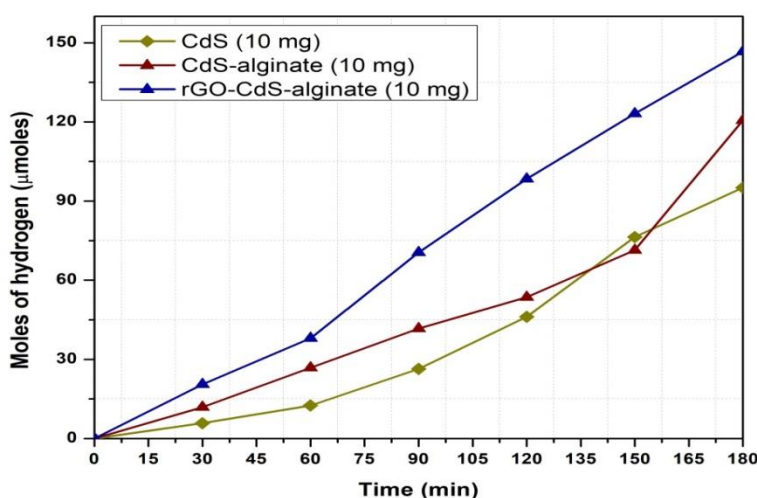


Fig-4.14 Comparative representation: Moles of hydrogen vs time plot using pristine CdS/ hybrid CdS-Sodium alginate and rGO-CdS-Sodium alginate with 10 mg of catalyst loading

4.2.4 Photocatalytic activity of different photo-catalyst:

Photo-catalyst is characterized by photocatalytic activity (moles of hydrogen generated/gm.of catalyst.hour). Activity plot of different photo-catalyst are shown below. From the bar plot it is clearly seen that activity of reduced graphene based CdS-Sodium alginate has maximum photocatalytic activity among synthesized photo-catalysts with 10 mg of catalyst loading.

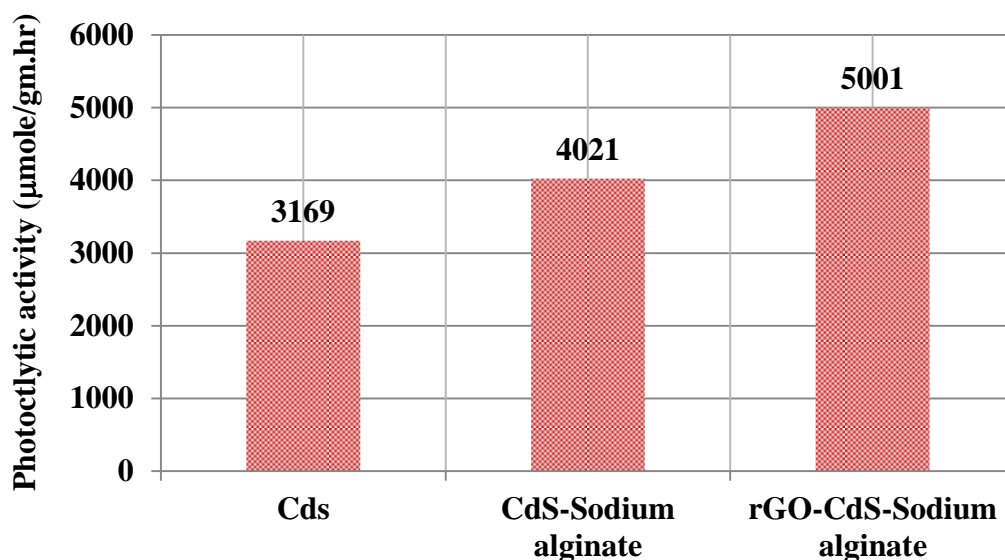


Fig-4.15 Activity (µmole/gm.hr) plot of different synthesized photo-catalysts (10 mg)

Catalyst name	Catalyst activity (µmoles/gm.hour)
Pristine CdS	3169
CdS-Sodium alginate	4021
rGO-CdS-Sodium alginate	5001

4.2.4 Study of change in catalyst loading for optimum photocatalytic activity

Among three catalysts, reduced Graphene oxide based CdS-Sodium alginate photocatalyst has better photocatalytic activity. So, further investigation is carried out for optimum performance. With increasing catalyst loading hydrogen generation is enhanced and reached at an optimum value 180.87 µmoles with catalyst loading 40 mg. with 15 ml of water.

Catalyst loading	10 mg	20 mg	30 mg	40mg
Time (min)	Moles of H ₂ (μmole)	Moles of H ₂ (μmole)	Moles of H ₂ (μmole)	Moles of H ₂ (μmole)
0	0	0	0	0
30	20.5	23.67	27.9	33.21
60	38.01	59.71	66.62	70.62
90	70.5	88.22	101.14	102.33
120	98.42	116.71	131.84	135.85
150	123.1	140.74	156.65	157.65
180	146.64	158.46	176.01	180.87

Graphical presentation: Performance analysis using rGO-CdS-Sodium alginate photocatalyst

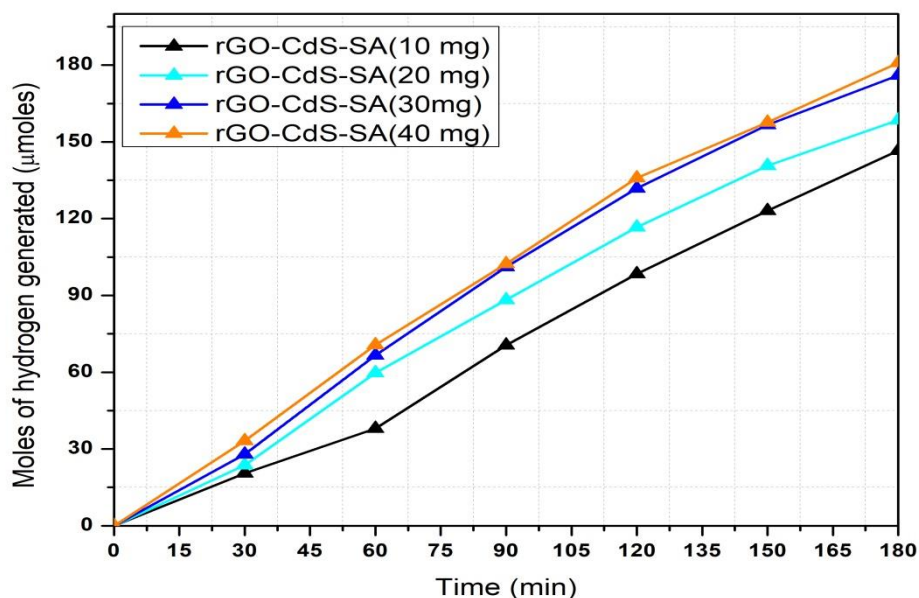


Fig-4.16 Moles of hydrogen generated vs time plot using rGO-CdS-Sodium alginate with different catalyst loading

Fig-4.16 shows that with increase in catalyst loading hydrogen generation increases. From 10 mg to 20 mg catalyst loading, hydrogen generation increases 11.82 μmoles and from 20 mg to 30 mg catalyst loading it increases 17.56 μmoles. But for 30 mg to 40 mg catalyst loading it increase

very small amount. From the figure it is clear that when catalyst loading changes from 30 mg to 40 mg rate of hydrogen generation curve coincides to each other that mean this 40 mg is the optimum catalyst loading.

Catalyst name	Catalyst loading	Photocatalytic activity ($\mu\text{moles/gm.hour}$)
	10 mg.	5001
rGO-CdS-Sodium alginate	20 mg.	5282
	30 mg.	5867
	40 mg.	6029

Photocatalytic activity of rGO-CdS-Sodium alginate photocatlyst with different catalyst loading:

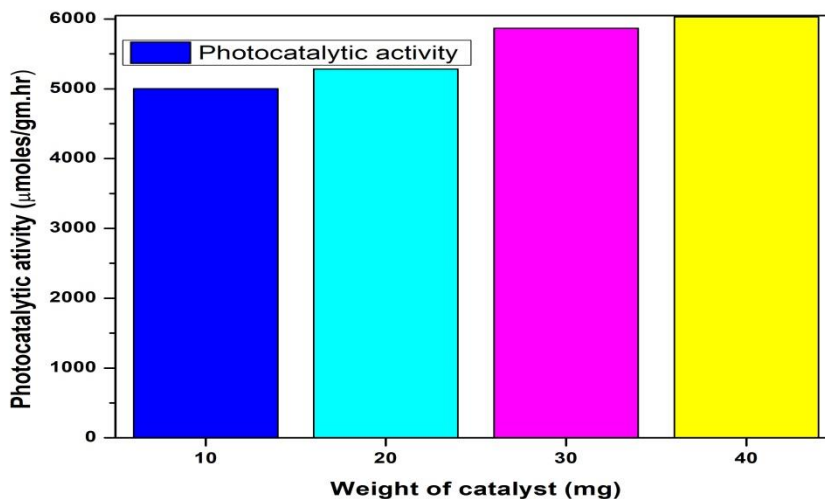


Fig-4.17 Photocatalytic activity plot of hybrid rGO-CdS-Sodium alginate with different loading

4.2.5 Kinetic study of photocatalytic water splitting

4.2.5.1 Kinetic model for photocatalytic water splitting using rGO-CdS-Sodium alginate

Step-1

Time (min)	Moles of H ₂ (μmole)	N _{A0} X _A	X _A (10 ⁻⁶)	N _A (moles of H ₂ O)	V _A (ml)	C _A (mole/ml)
0	0	0	0	0.833333	15	0.055555556
30	20.5	20.5	24.6	0.833316	15	0.055554417
60	38.01	38.01	45.612	0.833302	15	0.055553444
90	70.5	70.5	84.6	0.833275	15	0.055551639
120	98.42	98.42	118.104	0.833251	15	0.055550088
150	123.1	123.1	147.72	0.833231	15	0.055548717
180	146.64	146.64	175.968	0.833211	15	0.055547409

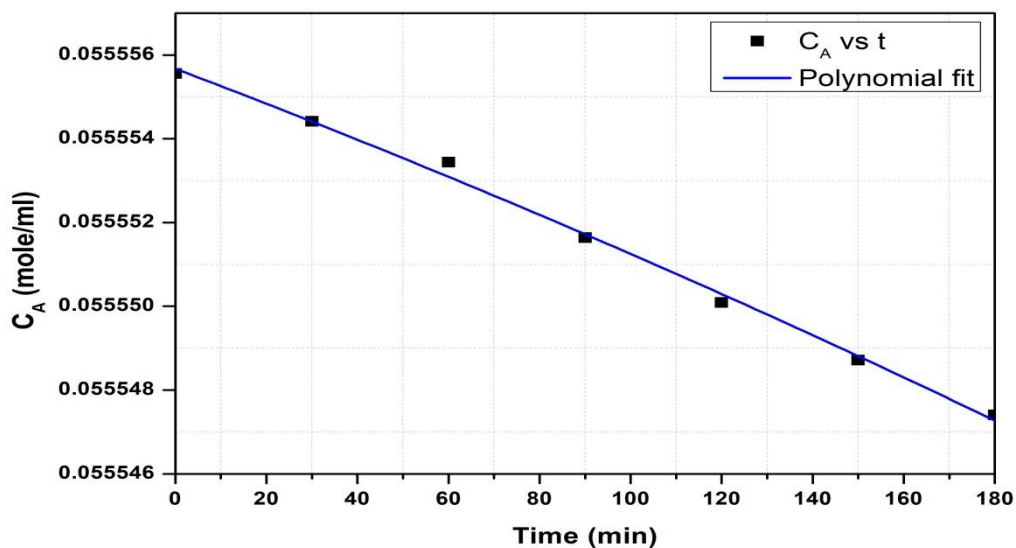


Fig-4.18 Concentration vs time plot

Second order polynomial equation fits with the experimental data. Equation is given below.

$$y = -3.08E-11x^2 - 4.11E-08x + 5.56E-02 \dots\dots\dots (4.2)$$

$$R^2 = 9.96E-01 \text{ (Fitness of curve)}$$

Equation in terms of C_A and t : $C_A = -3.08E-11t^2 - 4.11E-08t + 5.56E-02$ (4.3)

Step-2

Rate of the reaction (r_A): $(-dC_A/dt) = -[-2*3.08E-11t - 4.11E-08]$ (4.4)

Time (min)	Rate of the reaction (r_A)	Concentration (C_A)
0	4.11E-08	0.055555556
30	4.2948E-08	0.055554417
60	4.4796E-08	0.055553444
90	4.6644E-08	0.055551639
120	4.8492E-08	0.055550088
150	5.034E-08	0.055548717
180	5.2188E-08	0.055547409

Step-3

$1/(-r_A)$	$1/C_A$
-24330900	18
-23283971	18.000369
-22323422	18.0006842
-21438985	18.0012691
-20621958	18.0017717
-19864919	18.0022161
-19161493	18.0026399

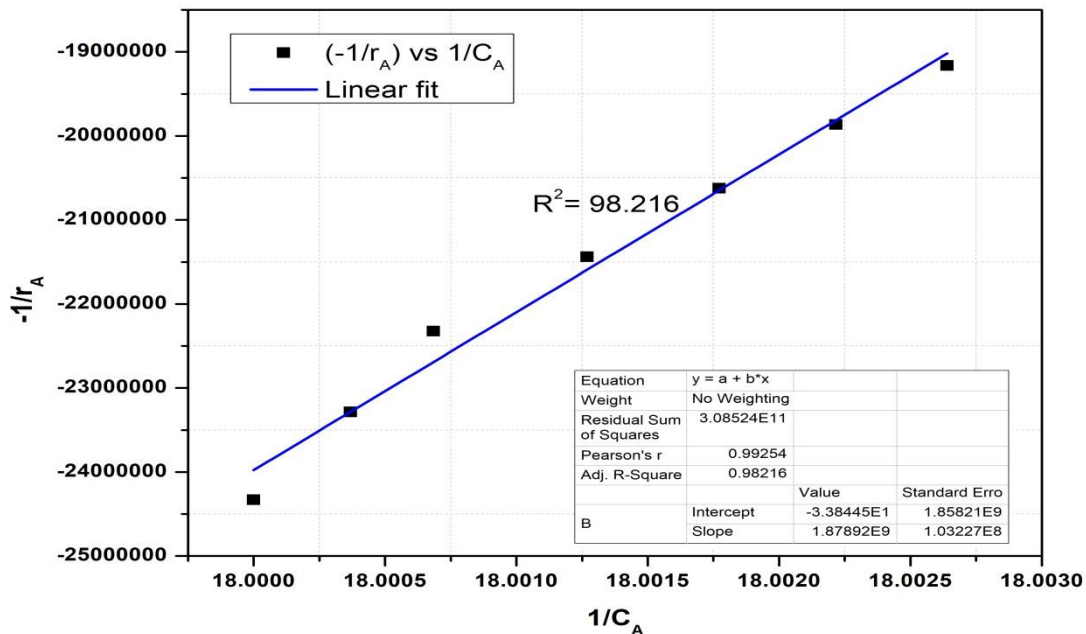


Fig-4.19 $1/(-r_A)$ vs $1/C_A$ plot

From the fig-4.19 it can be seen that fitness of the curve is 98% ($R^2=0.98$) so it satisfies our predicted rate equation. As photo-catalytic water splitting is a surface catalyzed reaction with adsorption it follows L-H kinetic model using rGO-CdS-Sodium alginate hybrid photo-catalyst.

4.2.5.2 Kinetic study of photocatalytic water splitting using CdS-Sodium alginate

Step-1

Time (min)	Moles of H ₂ (μmole)	N _{A0} X _A	X _A (10 ⁻⁶)	N _A	V _A (ml)	C _A (mol/ml)
0	0	0	0	0.833333333	15	0.055555556
30	11.9	11.9	14.28	0.833323417	15	0.055554894
60	26.78	26.78	32.136	0.833311017	15	0.055554068
90	41.66	41.66	49.992	0.833298617	15	0.055553241
120	53.52	53.52	64.224	0.833288733	15	0.055552582
150	71.42	71.42	85.704	0.833273817	15	0.055551588
180	120.63	120.63	144.756	0.833232808	15	0.055548854

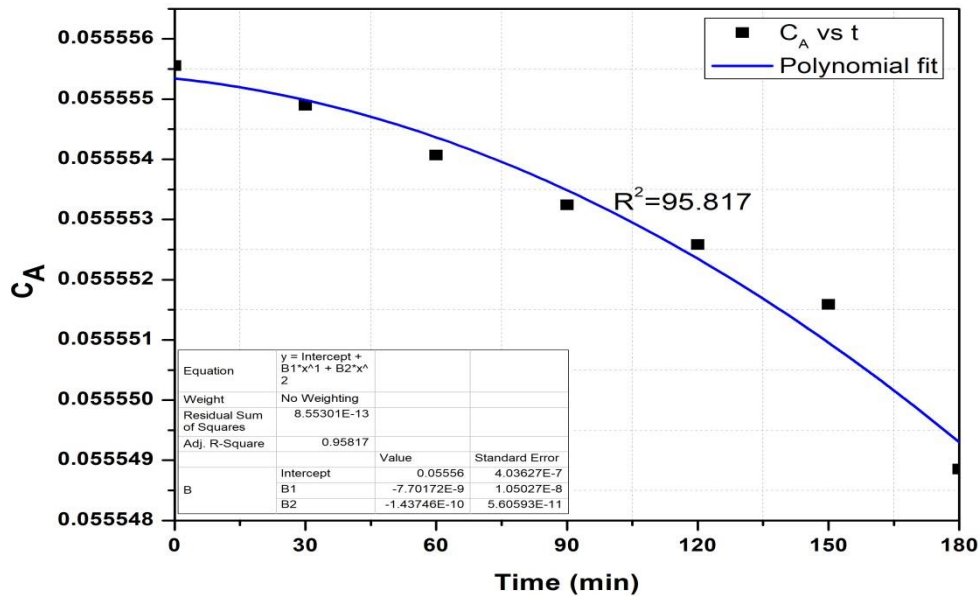


Fig- 4.20 Concentration vs time plot

Second order polynomial equation fits with the experimental data. Equation is given below:

$$y = -1.44\text{E-}10x^2 - 7.70\text{E-}09x + 5.56\text{E-}02 \dots\dots\dots (4.5)$$

$$R^2 = 9.72\text{E-}01$$

Equation in terms of C_A and t :

$$C_A = -1.44\text{E-}10t^2 - 7.70\text{E-}09t + 5.56\text{E-}02 \dots\dots\dots (4.6)$$

Step-2

Rate of the reaction (r_A): $(-dC_A/dt) = -[-2 \times 1.44 \times 10^{-10}t - 7.70 \times 10^{-9}] \dots\dots\dots (4.7)$

$-1/r_A$	$1/C_A$
-129870130	0.055556
-61199510	0.055555
-40032026	0.055554
-29744200	0.055553
-23663038	0.055553
-19646365	0.055552
-16795432	0.055549

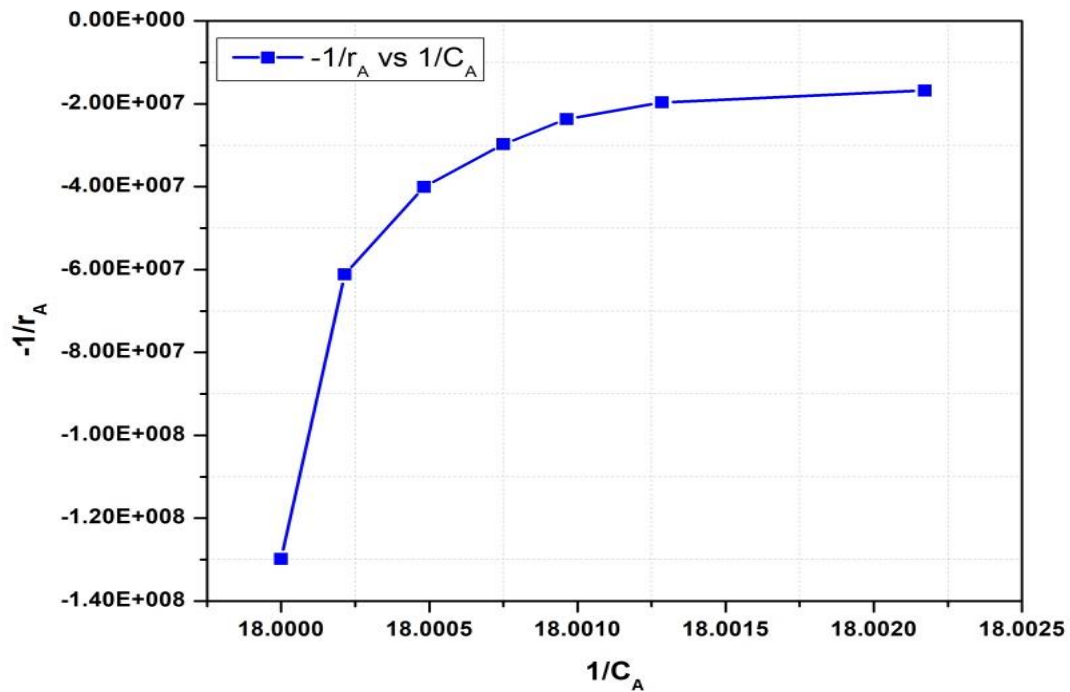


Fig-4.21 $(-1/r_A)$ vs $(1/C_A)$ plot

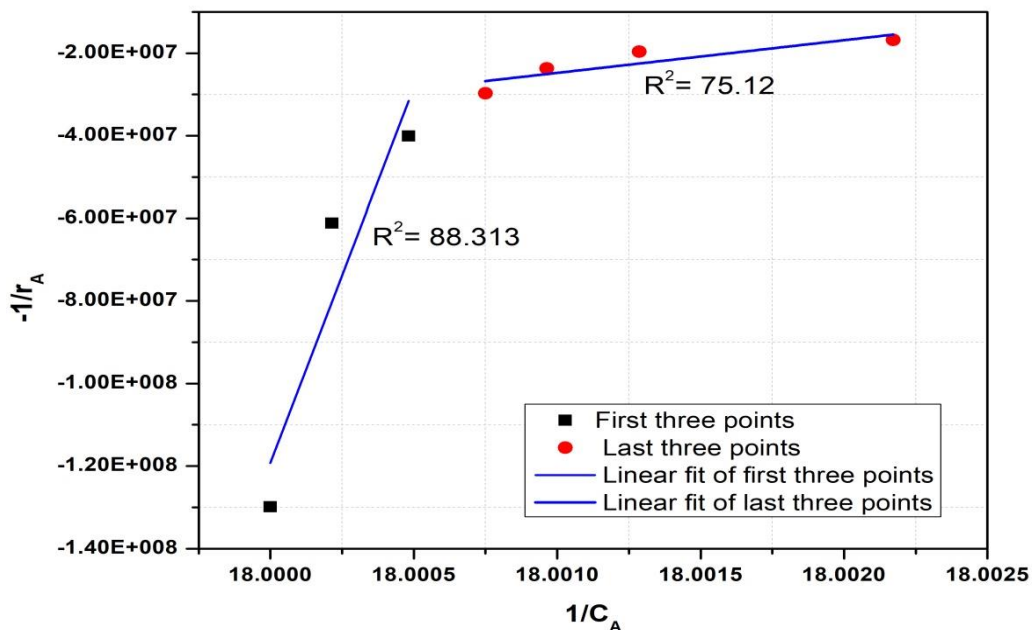


Fig- 4.22 ($-1/r_A$) vs $1/C_A$ plot in a splitting manner

From the fig- 4.21 it can be seen that all the points doesn't pass through straight line. So, this plot is divided into two parts that is depicted in Fig- 4.22. One part encompasses initial three points and other part involves last four points. Separately two parts of the curve are fitted with linear fit and R^2 value of two parts is 0.88 and 0.75 respectively. Therefore, it can be concluded that hydrogen production by photocatalytic water splitting follows L-H model for certain period of time initially but after certain period of time, the nature of the $1/(-r_A)$ vs $1/C_A$ plot does not fit well with the L-H model. So, it can be said that because of recombination, L-H model doesn't fit throughout the process. But using rGO this problem is totally omitted because presence of Graphene it reduces the rate of recombination and total process follows L-H model that is depicted in Fig- 4.19.

4.2.6 Study of recyclability of the photo-catalyst (rGO-CdS-Sodium alginate)

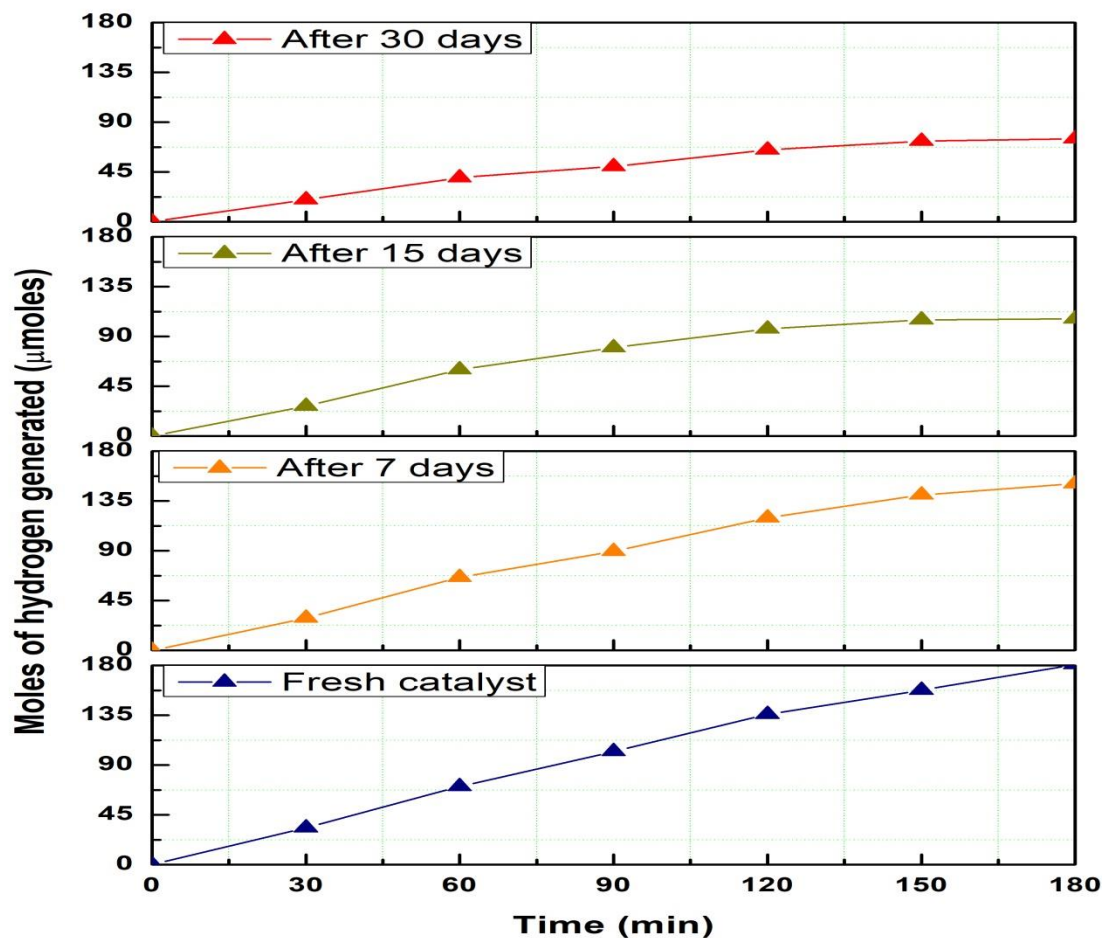


Fig-4.23 Effect of catalyst deactivation on moles of hydrogen generation for rGO-CdS-Sodium alginate

From the figure- 4.23 it can be seen that catalyst is deactivated with the passage of time. For fresh catalyst (rGO-CdS-Sodium alginate), 180.87 μmoles of hydrogen is generated during 3 hour operation. After 7 days, 15days and 30 days 150.7 μmoles , 106.89 μmoles and 75.04 μmoles of hydrogen is generated respectively during three hours operation with sama operational condition. Catalytic activity decreases from 6029 $\mu\text{moles/gm.hours}$ (fresh catalyst) to 2500 $\mu\text{moles/ gm.hours}$ (after 30 days).

CHAPTER-V

Conclusion

5.1 Conclusions

A highly active, reduced Graphene oxide based water adsorbent (Sodium alginate) mediated visible light active hybrid photo-catalyst named as rGO-CdS-Sodium alginate is proposed for enhanced hydrogen production by photocatalytic water splitting. The study of comparative analysis of photocatalytic activity is examined using three different synthesized photo-catalyst with 10 mg of catalyst loading, - Pristine CdS (3169 $\mu\text{moles/gm.hr}$), CdS-Sodium alginate (4021 $\mu\text{moles/gm.hr}$) and rGO-CdS-Sodium alginate (5001 $\mu\text{moles/gm.hr}$). Study on change of catalyst loading for optimum photocatalytic activity is also examined by varying catalyst loading. Here we report 40 mg of catalyst loading is the optimal value for 15 ml of water splitting. Also we have examined recyclability of photocatalytic activity (2500 $\mu\text{moles/gm.hr}$) and kinetic study of water splitting using rGO based CdS-Sodium alginate photo-catalyst. These catalyst are synthesized by different chemical methods and characterized by Scanning electron microscopy (SEM), Fourier transformed spectroscopy (FTIR), X-ray diffraction (XRD) and UV-VIS spectroscopy. XRD analysis reveals that grain size of synthesized catalyst is 9 nm. to 10 nm. In case Graphene supported catalyst the electron transport increases, which may enhances the photocatalytic activity. The experimental results of photocatalytic water splitting reveal that use of water adsorbent and Graphene- CdS-Sodium alginate and rGO-CdS-Sodium alginate catalysts enhances the rate of hydrogen generation ~ 20% and 36%, respectively compare to pristine CdS. Kinetic study of water splitting using rGO based CdS-Sodium alginate shows that it follows L-H model.

References

- [1] Eugene D. Coyle and Richard A. Simmons, 2014, **Understanding the Global Energy Crisis** Purdue University Press
- [2] **Overview of Renewable Power Generation**, Central Electricity Authority Reports, 2017
- [3] A. Fujishima and K. Honda **Electrochemical Photolysis of Water at a semiconductor electrode** Nature 238 (1972) 37-38
- [4] T N Veziroglu, S. Sahin, **21st century's energy: hydrogen energy system** Energy Conversion and Management 49 (2008) 1820-31
- Qin Li, Beidou Guo, Jianguo Yu, Jingrun Ran, Baohong Zhang, Huijuan Yan, and Jian Ru Gong, **Highly Efficient Visible-Light-Driven Photocatalytic Hydrogen Production of CdS-Cluster-Decorated Graphene Nanosheets**, J. Am. Chem. Soc. 2011, 133, 10878–10884
- [5] R.M.Navarro, F.del Valle, J.A.Villoria de la Mano, M.C.Álvarez-Galván, J.L.G.Fierro, **Photocatalytic Water Splitting Under Visible Light: Concept and Catalysts Development**, Adv Chem Eng, 36 (2009), pp. 111-143
- [6] Feriel Bouhjar, Bernabé Marí, Brahim Bessaïs, **Hydrothermal fabrication and characterization of ZnO/Fe₂O₃ heterojunction devices for hydrogen production**, J Anal Pharm Res. 2018;7(3):315–321
- [7] XinnianXia, YingzhuangXu, YouChen, YutangLiu, YanbingLu, LuhuaShao, Fabrication of MIL-101(Cr/Al) with flower-like morphology and its catalytic performance, Appl. Catal. A Gen., 559 (2018), pp. 138-145
- [8] Anagh Bhaumik and Jagdish Narayan, **Reduced Graphene Oxide-Nanostructured Silicon Photosensors with High Photoresponsivity at Room Temperature**, ACS Appl. Nano Mater.2019242086-2098
- [9] François Perreault, Andreia Fonseca de Faria and Menachem Elimelech, **Environmental applications of graphene-based nanomaterials**, Chem. Soc. Rev., 2015, 44, 5861--5896
- [10] Filippo Giannazzo, Sushant Sonde and Vito Raineri, **Electronic Properties of Graphene Probed at the Nanoscale**

- [11] Yingchun Yu, Youxian Ding, Shengli Zuo, and Jianjun Liu, **Photocatalytic Activity of Nanosized Cadmium Sulfides Synthesized by Complex Compound Thermolysis**, *Int J Photoenergy*. 2011 (2010) 1-5
- [12] Daniela C. Marcano et al. , **Improved Synthesis of Graphene Oxide**, *ACS Nano* 4 (2010) 4806-4814
- [13] Sudhir Ramprasad, Yu-Wei Su, Chih-Hung Chang, Brian K. Paul and Daniel R. Palo **Continuous Microreactor-Assisted Solution Deposition for Scalable Production of CdS Films**, *ECS Journal of Solid State Science and Technology*, 2 (9) P333-P337 (2013)
- [14] Petr Zamostny, Zolenk Belohlav, **Identification of kinetic models of heterogeneously catalyzed reactions**, *Applied Catalysis A: General* 225 (2002) 291–299
- [15] [OCTAVE_LEVENSPIEL] **CHEMICAL REACTION ENGINEERING 3TH EDITION**
- [16] Muneerah Alomar, Yueli Liu and Wen Chen, **Surface Decorated Zn_{0.15}Cd_{0.85}S Nanoflowers with P25 for Enhanced Visible Light Driven Photocatalytic Degradation of Rh-B and Stability**, *Appl. Sci.* 8 (2018) 327-341
- [17] Chengling Jiang, Zhiliang Wang, Xueqin Zhang, Xiaoqun Zhu, Jun Nie and Guiping Ma, **Crosslinked polyelectrolyte complex fiber membrane based on chitosan–sodium alginate by freeze-drying**, *RSC Adv.* 4 (2014) 41551-41560
- [18] Qin Li, Beidou Guo, Jiaguo Yu, Jingrun Ran, Baohong Zhang, Huijuan Yan, and Jian Ru Gong, **Highly Efficient Visible-Light-Driven Photocatalytic Hydrogen Production of CdS-Cluster-Decorated Graphene Nanosheets**, *J. Am. Chem. Soc.* 133 (2011) 10878–10884
- [19] Jiahong Wang, Shan Liang, Liang Ma, Sijing Ding, Xuefeng Yu, Li Zhou and Ququan Wang, **One-pot synthesis of CdS–reduced graphene oxide 3D composites with enhanced photocatalytic properties**, *Cryst Eng Comm*, 16 (2014) 399-405
- [20] Francisco Tiago Leitaõ Muniz, Marcus Aure´lio Ribeiro Miranda, Ca´sio Morilla dos Santos and Jose´ Marcos Sasaki, **The Scherrer equation and the dynamical theory of X-ray diffraction**, *Acta Cryst.* (2016). A72, 385–390

